U.PORTO

FEUP FACULDADE DE ENGENHARIA UNIVERSIDADE DO PORTO

a4f algae for future

Mestrado Integrado em Bioengenharia

Rapid detection of contaminant microorganisms in microalgae reactors

Dissertação de Mestrado em Engenharia Biológica

Joana Isabel Pinheiro da Silva Pinto

Desenvolvida no âmbito da unidade curricular de Dissertação

Orientador na FEUP: **Prof. Nuno Azevedo**

Orientador na A4F: **Dr. Tiago Guerra**

Porto, Junho 2017

Acknowledgements

I would like to express my extreme gratitude to Professor Nuno Azevedo and Dr Tiago Guerra, not only for making this association between the university and a company possible, which allowed me to experience a different environment, but also for the support and guidance throughout this thesis development.

I would also like to thank Andreia Azevedo and Noreen Heigle for being always so kind and available to help me with any problems faced during this project.

Somehow this thesis ends a chapter of my life, one that I couldn't go through without the support of my friends and family, who constantly reminded me to focus on what really matters and gave me strength to overcome every day struggles.

To Catarina, Patrícia, Sara, Jessica and Diana, my biochemical companions, I am so lucky to have you as my best friends. Fortunately, during our journey we ended up joining and starting this amazing group. It really doesn't matter how far we are, physically, from each other. Our sisterhood keep us together no matter what challenge us.

To Ayala, Filipe, Mata and Zé, thank you for your friendship and the most fun board gaming nights. Thank you, Ayala, for your simplest explanations for my biological doubts. Thank you, Filipe, for your companionship, it was indeed a fun coincidence to found out that you live and work near me, thank you for making my home walks less tedious. Mata, you are indeed unique, thank you for the best talks and the best cakes. Zé, thank you for always pushing me to go higher and further, not only during our climbing days, but also in my daily challenges in life.

I would also like to thank my Oporto family, thank you Inês and Sílvia for being the most hilarious roommates. I will miss our dinners and workout sessions. To Isabel and family and to Maria João and family, I want to express my gratitude for always hosting me with the best conditions and for making me always feel like home. Thank you for helping me in the most random situations. Thank you for your care and friendship.

Finally, to my family, especially to my parents and my brother, there are not enough words to express my gratitude. Thank you for your support, encouragement and endless love throughout these years.

Prof. Nuno Azevedo, supervisor of this work, is a member of LEPABE – Laboratório de Engenharia de Processos, Ambiente, Biotecnologia e Energia, funded by Projects (i) POCI-01-0145-FEDER-006939 (Laboratório de Engenharia de Processos, Ambiente, Biotecnologia e Energia, UID/EQU/00511/2013) - funded by FEDER through COMPETE2020 - Programa Operacional Competitividade e Internacionalização (POCI) – and by national funds through FCT - Fundação para a Ciência e a Tecnologia and (ii) NORTE-01-0145-FEDER-000005 – LEPABE-2-ECO-INNOVATION, funded by FEDER - Fundo Europeu de Desenvolvimento Regional, through COMPETE2020 – Programa Operacional Competitividade e Internacionalização (POCI) and Programa Operacional Regional do Norte (NORTE2020)

Abstract

The microalgae *Haematococcus pluvialis* is the best source for natural astaxanthin production, since *H. pluvialis* can accumulate astaxanthin up to 4% of dry weight. Astaxanthin is a powerful antioxidant with applications in the medical and nutraceutical industries. However, the mass cultivation of this microalgae is threatened by a blastoclad parasite, *Paraphysoderma sedebokerense,* which has a devastating effect due to the fast collapse they cause on *Haematococcus* populations.

One of the major issues faced during microalgae production is hence to maintain a pathogen-free production system and finding ways to control microbial contaminations in the photobioreactors. To evaluate the quality of microalgae production it is common to use plating methods, which take up to 3 days to provide results, or polymerase chain reaction (PCR)-based methods, which implies the extraction of nucleic acids from the cells.

To allow a rapid response when contaminations occurs it is urgent to find other methods. During this thesis, a peptide nucleic acid-based probe (PNA) was designed to rapidly detect the contaminant microorganism through fluorescence *in situ* hybridization, which unlike PCR-based methods allows the detection of specific nucleic acid sequences in whole cells.

The theoretical specificity and sensitivity of the PNA probe were both 100%. The best temperature for the hybridization was found to be close to 55ºC with a significant difference to temperatures lower than 52 ºC or higher than 58 ºC. The method was successfully adapted for the detection of *P. sedebokerense* in mixed cultures with *Haematococcus* by fluorescence microscopy and the detection limit was found to be lower than 10 infected *Haematococcus* cells/mL.

Routine monitoring and early detection of contaminant species is a clear requirement for large-scale cultivation. The PNA-FISH method would undoubtedly benefit the detection of the fungal parasite in *H. pluvialis* cultures.

Keywords: *in situ* hybridization; FISH; PNA; Peptide nucleic acid; *Paraphysoderma sedebokerense*.

Resumo

A microalga *Haematococcus pluvialis* é a melhor fonte de produção natural de astaxantina, conseguindo acumular quantidades superiores a 4% do seu peso seco. A astaxantina é um antioxidante com aplicações nas indústrias farmacêuticas e alimentares. Contudo, o cultivo desta microalga à escala industrial é ameaçado por um fungo do filo Blastocladiomycota, *Paraphysoderma sedebokerense*, que tem um efeito nefasto nas culturas, levando a um rápido colapso das populações de *Haematococcus.*

Um dos principais problemas aquando do processo de produção de microalgas é a manutenção de sistemas livres de agentes contaminantes e encontrar formas de controlar as contaminações nos fotobioreatores. De forma a avaliar a qualidade da produção de microalgas é comum recorrer-se a métodos de plaqueamento, que podem demorar mais de 3 dias a ceder resultados, ou métodos moleculares baseados na técnica de reação em cadeia da polimerase (PCR) que requerem a extração dos ácidos nucleicos das células.

De forma a detetar rapidamente a ocorrência de contaminantes é urgente desenvolver novos métodos. Durante esta tese, uma sonda de ácido nucleico peptídico (PNA) foi desenvolvida de forma a detetar-se rapidamente o parasita *P. sedebokerense* a partir de hibridação de fluorescência *in situ*, que, ao contrário dos métodos moleculares à base de PCR, não necessita da extração do conteúdo de ácidos nucleicos, uma vez que a deteção se dá diretamente na célula.

A especificidade e sensibilidade teórica da sonda é de 100%. As condições de hibridação foram otimizadas e a temperatura ótima para a hibridação ronda os 55 ºC com diferença significativa para temperaturas inferiores a 52 ºC ou superiores a 58 ºC. A técnica foi adaptada com sucesso para a deteção do fungo parasita *P. sedebokerense* em culturas mistas com *Haematococcus pluvialis* a partir de microscopia de fluorescência, sendo o seu limite de deteção inferior a 10 células de *Haematococcus* infetadas/mL.

Para a produção em grande escala é necessário um controlo diário e uma rápida deteção de contaminantes. O método de PNA-FISH demonstrou-se claramente benéfico para a deteção do parasita *P. sedebokerense* em culturas de *H. pluvialis*.

Palavras Chave: hibridação *in situ*; FISH; PNA; ácido nucleico peptídico; *Paraphysoderma sedebokerense*

Declaração

Declara, sob compromisso de honra, que este trabalho é original e que todas as contribuições não originais foram devidamente referenciadas com identificação da fonte.

List of Contents

Work outline **1**
1.1. Introduction **1**
1.2. Research objectives **1**
1.3. Thesis organization **2**
Literature review **4**
2.1. Production of astaxanthin by Haematococcus pluvialis **4**
2.2. Contamination of Haematoccocus pluvialis by Paraphysoderma sedebokerense **5**
2.3. Detection of contaminants in algae cultures **7**
2.4. Fluorescence in situ Hybridization **8**
2.4.1. Fluorescence in situ Hybridization: Technical Aspects 9
2.4.2. Drawbacks 11
2.5. Nucleic Acid Mimics: Peptide Nucleic Acids (PNA) **13**
Materials and Methods **15**
3.1. Culture maintenance **15**
3.1.1. Paraphysoderma sedebokerense culture 15
3.1.2. Haematococcus pluvialis culture 15
3.1.3. Paraphysoderma-infected Haematococcus cultures 15
3.2. In silico PNA probe design **15**
3.3. Theoretical evaluation of the PNA probe performance **16**
3.4. Hybridization procedure on glass slides **17**
3.5. Hybridization procedure on suspension **17**
3.6. WGA-Rhodamine staining **18**
3.7. Determination of the detection limit **18**
3.8. Microscopy Analysis **19**
3.9. Measurement of the intensity of fluorescence and statistics tests **20**
Results and discussion **21**
4.1. Probe design **21**
4.2. Determination of theoretical specificity and sensitivity **21**
4.3. Evaluation of autofluorescence and possible treatments **22**
4.4. Determination of the hybridization temperature **26**
4.5. WGA-Rhodamine staining **29**
4.6. Determination of the detection limits **30**
Concluding remarks and future work **32**
5.1. General conclusions 32
5.2. Future work 33
Bibliography **34**
Appendix A1. Culture media composition ..... **i**

Appendix A2. Designed probe characteristics ii
Appendix A3. Student's t Test for probe specificity testing v
Appendix A4. Statistics for protocol optimization viii
Appendix A5. Detection limit experiments xvi

List of figures

Figure 1. Schematic representation of Paraphysoderma sedebokerense life cycle.. 6
Figure 2. Number of citations in the PubMed database for the keywords "fluorescence in situ hybridization" by year 9
Figure 3. Scheme of the fluorescence in situ hybridization method 11
Figure 4. Schematic representation of DNA and PNA chemical structure. 14
Figure 5. The relative transmittance intensity values of excitation filter and emission filter of the U-FBN filter. Fluorescence spectra of the fluorophore 5-FAM 19
Figure 6. Specificity test for Saccharomyces cerevisae and Haematococcus pluvialis 23
Figure 7. Intensity of fluorescence for Haematococcus pluvialis and Saccharomyces cerevisae with and without the probe..... 24
Figure 8. Paraphysoderma sedebokerense reduction treatment with UV photobleaching 24
Figure 9. Paraphysoderma sedebokerense reduction treatment by freezing at -80ºC 25
Figure 10. Paraphysoderma sedebokerense reduction treatment with Trypan Blue 25
Figure 11. Paraphysoderma sedebokerense reduction treatment with UV photobleaching and with Trypan Blue 26
Figure 12. Compatibility of autofluorescence reduction treatment with Sudan Black B and fluorescence in situ hybridization using a PNA-probe 26
Figure 13. Intensity of fluorescence normalized for temperatures between 50 and 60 ºC, with and without the probe. 288
Figure 14. WGA-Rhodamine staining at Haematococus infected by Paraphysoderma sedebokerense. 299
Figure 15. Example of a H. pluvialis infected cell by two P. sedebokerense cells. 30
Figure 16. Percentage of infection versus a dilution factor with healthy Haematococcos pluvialis. 3131
Figure 17. Haematotoccus pluvialis infected with Paraphysoderma sedebokerense. 31

Figure A5 1. Dilution curves of Haematococcus infected cultures with PS1 and PS2 strains xvi

List of tables

Table 1. Characteristics of the selected probe and their values 21
Table 2. ANOVA test for the comparison between different temperatures of hybridization 27

Table A1 1. Paraphysoderma sedebokerense and Haematococcus pluvialis growth medium composition i

Table A2 1. Complementary sequences to the designed PNA-probe ii

Table A3 1. Shapiro-Wilk' test of normality for the samples of Saccharomyces cerevisae, treated with the probe and without the probe. v
Table A3 2. Shapiro-Wilk' test of normality for the samples of Haematococcus pluvialis, treated with the probe and without the probe. v
Table A3 3. Statistics description for samples of Haematococcus pluvialis treated with and without the probe v
Table A3 4. Statistics information for the intensity of fluorescence of Saccharomyces cerevisae treated with and without the probe. vi
Table A3 5. Statistics information for the intensity of fluorescence of Haematococcus pluvialis treated with and without the probe. vi
Table A3 6. Student's t Test between the samples with and without the probe for Saccharomyces cerevisae vi
Table A3 7. Student's t Test between the samples with and without the probe for Haematococcus pluvialis vii

Table A4 1. Shapiro-Wilk' test of normality for the samples at different temperatures from 50 to 60 ºC, treated with the probe viii
Table A4 2. Statistics description for samples at different temperatures treated with the probe viii
Table A4 3. Mauchly's Test of Sphericity for the samples treated with the probe x
Table A4 4. Tests of Sphericity for the samples treated with the probe xi
Table A4 5. Statistics information for the different temperatures treated with the probe xi
Table A4 6. ANOVA test between the different temperatures xi
Table A4 7. Shapiro-Wilk' test of normality for the samples at different temperatures from 50 to 60 ºC, non-treated with the probe xii
Table A4 8. Statistics description for samples at different temperatures treated with the probe. xiii
Table A4 9. Statistics information for the different temperatures treated with and without the probe. xv
Table A4 10. Student's t Test between the samples with and without the probe for the different temperatures. xv

Table A6 1. Detection limit [cells/mL] according to the calibration curves obtained and the value of total infected cells. xvii

Glossary

Abbreviations

A4F	Algae for Future, S.A.
ANOVA	Analysis of variance
bp	Base pair
CO_2	Carbon dioxide
DNA	Deoxyribonucleic acid
e.g.	for example
FISH	Fluorescence *in situ* hybridization
H.	*Haematococcus*
ISH	*In situ* hybridization
Ku	Kurtosis
LSD	Least Significant Difference
NCBI	National Centre for Biotechnology Information
nPs	Non-*Paraphysoderma sedebokerense* strains that did not react with the probe
RNA	Ribonucleic acid
rRNA	Ribosomal ribonucleic acid
P.	*Paraphysoderma*
PBS	Phosphate-buffer saline
PCR	Polymerase chain reaction
PNA	Peptide nucleic acid
PS	*Paraphysoderma sedebokerense*
sig.	Significance
Sk	Skewness
sp.	Specie
spp.	Species
Tm	Melting temperature
tPs	Total of non-*Paraphysoderma sedebokerense* strains
ts	Theoretical specificity
UV	Ultraviolet
vol	Volume
WGA	Wheat germ agglutinin
wt	Weight

Chapter 1

Work outline

1.1. Introduction

Microalgae are photosynthetic microorganisms that produce biomolecular compounds as result of photosynthesis. Under specific stress condition, microalgae can accumulate, beside lipids and carbohydrates, considerable amounts of secondary metabolites with high industrial value. One of the most valuable algal compounds is astaxanthin, a ketocarotenoid pigment with many applications that range from animal feed, cosmetics, pharmaceutics and nutraceuticals (Borowitzka 2013; Cardozo et al. 2006; Koller et al. 2014; Pérez-López et al. 2014). Several microalga genera such as *Chlorella sp.* (Del Campo et al. 2004), *Chlorococcum sp.* (Ma & Chen 2001) or *Scenedesmus sp.* (Qin et al. 2008) are reported as potential producers of astaxanthin. However, the freshwater green microalgae *Haematococcus pluvialis* productivity yield exceeds any other known source, once *H. pluvialis* can accumulate astaxanthin over 4% of its dry weight (Boussiba 2000; Boussiba & Vonshak 1991). Since *H. pluvialis* is the most productive source of natural astaxanthin production, the interest in this particular microalga, for commercial cultivation, has increased. Consequently, microbial contaminants that harm their production by reducing biomass yield and quality received also a great attention recently (Shah et al. 2016). *H. pluvialis* is reported to be contaminated by fungal parasites and zooplanktonic predators, such as amoebas, ciliates and rotifers, as well as other microalgae and cyanobacteria (Han et al. 2013). Among these, fungal contamination by chytrids has been recognized as one of the most serious impediments for astaxanthin production. One of these parasitic chytrid fungus is *Paraphysoderma sedebokerense*, which is responsible for astaxanthin production reduction and frequently leads *Haematococcus* cultures to collapses (Hoffman et al. 2008; Strittmatter et al. 2016).

Rapid detection of contaminants is necessary for the prevention and control of microbial contamination is microalgae cultures. Methods of detection usually include microscopy and staining, flow cytometry, molecular-based detection by polymerase chain reaction (PCR)-based methods (Shah et al. 2016).

1.2. Research objectives

The main goal of this work was to develop a rapid way to detect contaminant microorganisms in microalgae reactors. In this particular case, the option was to detect the fungal parasite *P. sedebokerense* in *Haematococcus* cultures by fluorescence *in situ* hybridization (FISH). If applicable, the developed

technique could be used for industrial application on large scale *H. pluvialis*. This work comprised the following specific objectives:

- **Design a peptide nucleic acid (PNA)-based probe for *P. sedebokerense* detection by FISH:** The PNA probe was designed from 18S ribosomal RNA sequences of the fungal parasite *P. sedebokerense* available at GenBank. As a control, sequences of the closest relatives and other organisms that might be present on the photobioreactor were added to the dataset. Sequences were aligned to select possible regions for probe design and the selection of the probe sequence was based on regions that showed differences between the *P. sedebokerense* sequences and the non-target strains. Additionally, other selection criteria were used to select the PNA probe, such as: Gibbs free energy; pyrimidine content; presence of self-complementary structures and melting temperature.
- **Optimisation of the hybridization procedure:** Different parameters (e.g. hybridisation temperature and solutions, as well as, fixation and permeabilization steps in axenic cultures) were optimised with respect to fluorescence signal intensity and signal-to-noise ratio.
- **Test the procedure on *Haematococcus* cultures infected with *P. sedebokerense*:** the procedure was tested in mixed cultures and the detection limit determined.

1.3. Thesis organization

This work is divided in five chapters. In Chapter 1 the main goals, context, and motivations for this study are presented. The guideline for the overall work presented in the further chapters is also described.

Chapter 2 provides a brief review of the literature. The importance of microalgae production and their main applications are described, focusing on the major role that parasites have in hampering microalgal production. The chapter includes a description of the life cycle of the contaminant microorganism *P. sedebokerense* and the current methodologies that are employed to detect contaminant microorganisms. This is followed by the description of the technique that is used in this work, fluorescence *in situ* hybridization, which includes a description of its technical aspects and possible drawbacks. Further research led to the development of improved methods, such as the use of nucleic acid analogues, known as RNA/DNA mimics. In this work, a peptide nucleic acid probe was used. For that reason, there is also a description of their proprieties and importance.

Chapter 3 describes the Materials and Methods used during this work. There is a description of the culture maintenance, how the *in silico* PNA probe was designed, how the probe was evaluated in terms of its theoretical performance and the hybridization procedure on suspension. Additionally, there is also a description of the protocol used for autofluorescence reduction and for the determination of the detection limit. The detection of *P. sedebokerense* using wheat germ agglutinin (WGA)-Rhodamine was also tested.

In Chapter 4 the results are presented and discussed, regarding aspects such as the probe design, theoretical and experimental specificity and sensitivity tests, protocol optimization, WGA-Rhodamine staining and detection limit determination.

Finally, the Chapter 5 presents an overview of all the developed work, with prominence on the main conclusions, on the limitations and perspectives for further research.

Chapter 2

Literature review

2.1. Production of astaxanthin by *Haematococcus pluvialis*

Microalgae are prokaryotic or eukaryotic photosynthetic organisms with quite few requirements for growth. Through sunlight they can convert water and carbon dioxide (CO_2) into molecules such as proteins, amino acids, lipids, polysaccharides, carotenoids and other biologically-active compounds (Mulbry et al. 2008).

Microalgae are present in not just aquatic but also terrestrial ecosystems, representing a wide variety of species living in an extensive range of environmental conditions. More than 50,000 species are predicted to exist, but only a limited number of around 30,000 have been studied and analysed (Richmond 2004). They have the ability to fix CO_2 through solar energy with a 10 times greater efficiency than terrestrial plants. Due to their efficiency, fast growth, low greenhouse gas emissions and capability to live in harsh conditions they can be a promising biomass feedstock (Mostafa 2012; Wang et al. 2013; Brennan & Owende 2009). Also, microalgae have potentially many broad applications in biotechnology, including biofuel (Chisti 2007; Chiaramonti et al. 2015), pharmaceuticals and as feed in aquaculture (Mulbry et al. 2004). There is also a wide potential in areas such as human and animal nutrition, biofertilizers, cosmetics, and cancer therapy (Ibañez & Cifuentes 2013; Strittmatter et al. 2016).

One of many industrially interesting microalgae is *H. pluvialis* Flotow. *H. pluvialis* is a unicellular biflagellated green algae, belonging to the algal class Chlorophyceae. *H. pluvialis* is best known for producing large amounts of the ketocarotenoid astaxanthin when exposed to adverse conditions (Boussiba 2000) such as, nutrient limitation (Kakizono et al. 1992), photon irradiance (Koyabashi et al. 1992; Li et al. 2010), increased salinity (Sarada et al. 2002; Li et al. 2008), high/low temperatures (Tjahjono et al. 1994), and combinations of stress (Lemoine & Schoefs 2010; Margalith 1999; Fan et al. 1994). During stress conditions, *H. pluvialis* transforms into a non-motile palmelloid cell which further evolves into a resting cyst (aplanospore) with a tough cell wall. In this stage of the life cycle, it starts accumulating astaxanthin (Del Campo et al. 2007; Lorenz et al. 2000), a natural pigment considered to be one of the most valuable algal compounds (Panis & Rosales Carreon 2016), frequently used in cosmetics, pharmaceutics, nutraceuticals and animal feed (Strittmatter et al. 2016; Pérez-López et al. 2014; Koller et al. 2014; Borowitzka 2013; Cardozo et al. 2006).

The freshwater microalga *H. pluvialis* is the richest source of natural astaxanthin. Although over 95% of the astaxanthin consumed is synthetically derived astaxanthin, consumer demand for natural products makes the synthetic pigments much less desirable and provides an opportunity for the its natural

production by *Haematococcus* (Lorenz et al. 2000). There are over sixteen international companies cultivating *H. pluvialis* at large scale (Shah et al. 2016).

Astaxanthin ($C_{40}H_{52}O_4$, 3,3'-dihydroxy-β,β′-carotene-4,4′-dione) is a member of the xanthophyll family of carotenoids and is abundant in fresh and salt water (Zhang et al. 2014; Markou & Nerantzis 2013). It is known by the typical reddish colour it gives to salmonids like salmons or trouts. It is also responsible for the pigmentation of various aquatic organisms such as shrimps, lobsters and other crustaceans. For their coloration, these organisms are dependent on the supply with astaxanthin by microalgae phytoplankton. Furthermore, it displays a central role for their immune-system and positively impacts their fertility (Koller et al. 2014).

Astaxanthin is considered the most powerful antioxidant in nature, hence an extremely efficient scavenger of free radicals (Koller et al. 2014; Naguib 2000). It also protects the skin against UV-induced photo-oxidation and it is used for anti-tumour therapies and prevention/treatment of neural damage diseases such as Alzheimer and Parkinson (Cardozo et al. 2006; Zhang et al. 2007). Furthermore, this substance is considered as a natural nutraceutical supplement to improve athletic performance by increasing stamina and reducing the time of muscle recovery (Capelli et al. 2013).

The increasing levels of microalgae production at industrial-scale was joint by the appearance of pathogens that harm their production and lead to a strong interest in these contaminants (Carney & Lane 2014). Fungal contamination by chytrids has been recognized as one of the most serious impediments for natural astaxanthin production from the green algae *H. pluvialis* (Han et al. 2013).

2.2. Contamination of *Haematoccocus pluvialis by Paraphysoderma sedebokerense*

Hoffman *et al.* (2008) first described *P. sedebokerense,* as a "*Haematococcus* parasite", after it was discovered in *H. pluvialis* cultures in Israel. It was grouped to the Chytridiomycota, a group of fungal parasites that are extremely common in freshwater and that are able to infect algae. Their host ranges can be narrow, such as *P. sedebokerense* (Hoffman et al. 2008; Gutman et al. 2009) or wide, such as *Rhizophydium algavorum* (Gromov et al. 1999). They can produce motile life stages know as zoospores which grow either saprotrophically, parasitically or both (Carney & Lane 2014).

In 2011, Porter *et al.* established the new phylum *Blastocladiomycota* (Porter et al. 2011), which contained amongst others *Paraphysoderma* as well as the closely related plant pathogen genus *Physoderma* (James et al. 2011; Hoffman et al. 2008). *Paraphysoderma* was first differentiated from *Physoderma* by the absence of a motile spore (James et al. 2011). However, Strittmatter *et al*. (2016) observed under optimal conditions fast-swimming, transiently uniflagellated *P. sedebokerense* zoospores which quickly transformed into infectious amoeboid swarmers.

Hoffman *et al.* (2008) also established the major steps in *P. sedebokerense* complex life cycle (Fig. 1). Under favourable conditions, amoeboid swarmer cells settle, attach and encyst on the *Haematococcus*

host cells. During infection, the cyst develops into a vegetative sporangium that eventually releases a new generation of amoeboid swarmers that move via pseudopodia. Under unfavourable conditions, the parasite displays a second type of life cycle and forms a different type of sporangium, the so-called resting sporangium, which can be distinguished from the vegetative sporangium by a thicker cell wall and dark opaque appearance. These resting sporangia can be found on the surface of its algal host but can also grow saprophytically on nutrient agar. Transferred into more favourable conditions amoeboid swarmer cells are released.

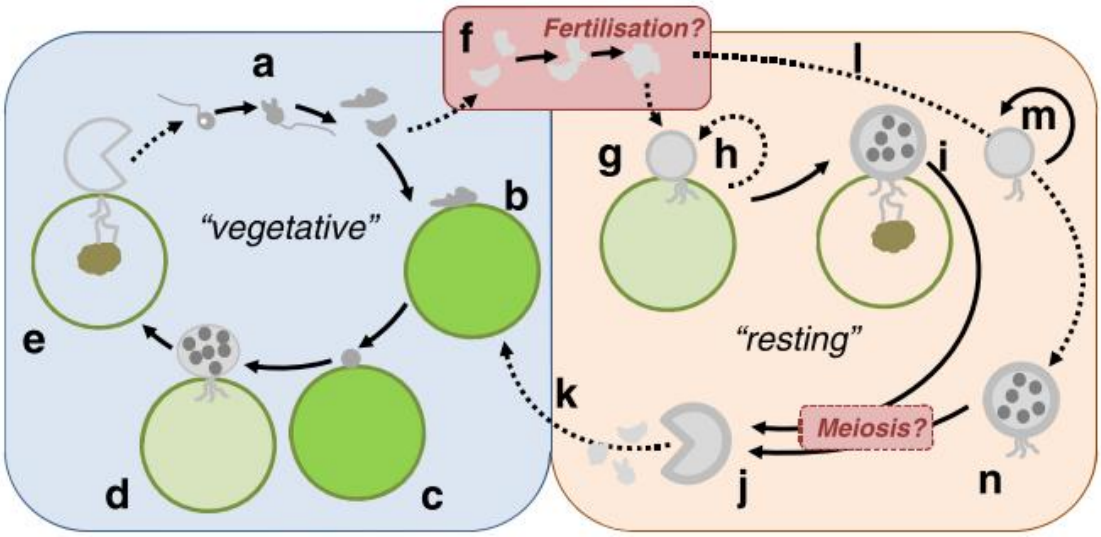

Figure 1. **Schematic representation of *Paraphysoderma sedebokerense* life cycle.** Vegetative, putative haploid phase (a-e): posteriorly uniflagellated zoospores (a) transition into infectious amoebae (b) that encyst at the surface of a host *H. pluvialis* (c). A rhizoid is formed inside the host and sustains the differentiation of a thin-walled sporangium (d), eventually releases a new generation of swarmer cells (e). A fertilization event between two amoebae possibly can lead to transition into the resting phase of the life cycle (f). Resting, putative diploid phase (g-h): in unfavourable growth conditions, the differentiating sporangium (g) originating from the encystment of a putative diploid amoeba can either undergo asexual reproduction (h) or evolve a thick wall and form a resting sporangium, still resulting in the death of the host cell (i). It is assumed that putative diploid amoebae can also grow saprophytically, e.g. on agar medium (l–n) and either undergoing asexual reproduction (m) or forming a resting sporangium (n) similar to (i). By analogy with the closely related genera *Physoderma* and *Urophlyctis*, meiosis occurs in the resting sporangia (Letcher et al. 2016) (i, n) giving rise to haploid swarmers (j). Transition between the vegetative (f) and resting (k) cycles would be triggered by fertilization and meiosis, respectively. Full and dotted arrows represent established and hypothesized life cycle transitions. Reprinted with permission from (Strittmatter et al. 2016).

In fact, *Paraphysoderma* has been discovered in several production facilities, and besides reducing astaxanthin production it is also responsible for frequent culture collapses (Hoffman et al. 2008; Gutman et al. 2009; Gutman et al. 2011). *Paraphysoderma* is a persistent problem in culture facilities, since as a chytrid fungus, produce cysts with thick-walls that resist to disinfection (Carney & Lane 2014). Recently, the interest in *Paraphysoderma* infection increased (Shin et al. 2001; Letcher et al. 2013; Carney et al. 2014; Chen et al. 2014) which lead to a number of patent applications in the USA and China aiming to control loss of biomass. This strongly suggesting that *P. sedebokerense* causes widespread production losses in industrial facilities across the world (Zhang et al. 2013; McBride et al. 2013).

2.3. Detection of contaminants in algae cultures

The detection of contaminants in industrial facilities is essential to prevent economic losses. Carney and Lane (2014) reviewed three ways to detect algal parasites. The first one combines Calcofluor white staining with fluorescence microscopy analysis to visualize chytrids by staining their chitin cell wall, present in certain life stages (Kagami et al. 2004; Rasconi et al. 2009). However, the Calcofluor white staining can be problematic for some algae, if cellulose is the primary cell wall component, as it is the case in *H. pluvialis*. Calcofluor white staining of cellulose and chitin may cause an ambiguous detection (Damiani et al. 2006). Additionally, Calcofluor white cannot stain fungus lacking chitin. The second technique to detect algal parasites is through flow cytometry. Flow cytometry is a technique for enumeration and characterization of suspended particles, usually in the 20 – 200 μM size range. Sieracki *et al.* (1998) have developed an automated flow cytometry and microscopy system known as FlowCAM (Fluid Imaging Technologies). The FlowCAM operates by streaming samples through a 3 x 3 mm glass chamber illuminated by a green laser, where relative fluorescence data, dimensions and a digital microscopic image of each particle are captured. Then, a software of image analysis carries out a pixel-based comparison correlation between captured images and a previously collected reference image setting the result in a percent similarity score. Images that exceed a user determined similarity score, are considered to match for the target organism and can be displayed for visual confirmation by the user for semiautonomous identification and enumeration of target species. FlowCam systems have been used in a diversity of applications in marine and aquatic sciences, including, the detection and enumeration of toxic dinoflagellate *Karenia brevis* in laboratory cultures, spiked natural phytoplankton assemblages and field samples from the Gulf of Mexico (Buskey & Hyatt 2006). Recently, FlowCam analysis has been applied to the monitoring of algal mass culture systems in order to detect algal predators (Day et al. 2012). A similar system was developed and demonstrated for the automated monitoring of cell count, size and morphology in microalgae culture (Havlik et al. 2013). The FlowCAM technology may be applicable to distinguish species visually. However, there are some methodological difficulties associated to the complexity of the chytrids life cycle. The major difficulties are related to the fact that chytrid zoospores have a small size (2-5 μm) (Canter & Jaworsky 1980) and the lack of phenotypic characteristics for easy identification and counting (Kudoh & Tokahashi 1990). Lastly, there are molecular-based detection and monitoring methods. Modern molecular methods used to detect parasites need an initial molecular identification which can be carried out by Sanger sequencing of isolated DNA samples or by shotgun approaches based on next generation sequencing technologies. Once identified and characterized, an oligonucleotide to target a specific region can be employed for the detection of parasitic species. Generally, the small subunit of the ribosomal RNA (rRNA) encoding region is the most used target since it contains both conserved and hypervariable regions used for phylogenetic analysis. Quantitative PCR (qPCR) is a powerful and widely employed detection method due to its high specificity to the target organism (Botes et al. 2013). A careful sample preparation (including primer design, validation, selection and testing the reagents) is required in order to limit background

contamination and achieve high levels of sensitivity. The qPCR reactions can be used to detect multiple species within a single reaction and have been used in commercial algae production to quantify changing densities of algae and their parasites in mass-culture, for example, *Amoeboaphelidium protocaccarum* (Letcher et al. 2013) and chytrids. Nonetheless, the equipment and reactions are very expensive (Shurin et al. 2013). In addition, it also implies the extraction of nucleic acids from the cells, unlike *in situ* hybridization which as it says, allows detection in whole cells. Due to its importance as a hybridization-based detection method, Fluorescence *in situ* Hybridization (FISH) is explained with detail in the next chapter.

2.4. Fluorescence *in situ* Hybridization

Fluorescence *in situ* hybridization is a powerful molecular technique that is used for a variety of purposes (Cerqueira et al. 2008; Amann et al. 1995; Amann et al. 1990; Guimarães et al. 2007; Wagner et al. 2003). The procedure consists on the detection of nucleic acids sequences through fluorescently-labelled nucleic acid probes which hybridizes specifically to the complementary target sequences within intact cells (Moter & Göbel 2000).

The first technique used to identify specific molecular identities was demonstrated by antigen-antibody interactions. In the early 1940s, antibodies were conjugated to fluorochromes without losing their epitope-binding specificity (Levsky & Singer 2003). In 1977, the first antibody-dependent fluorescent detection of nucleic acid hybrids was achieved (Rudkin & Stollar 1977). This technology was soon replaced by the development of fluorescent nucleic acid probes (Levsky & Singer 2003).

The earliest *in situ* hybridization (ISH), performed in the late 1960s, were not fluorescent, instead they used radioactive labelled probes (Pardue & Gall 1969; John et al. 1969). This technique allowed the examination of nucleic acid sequences without altering the morphology of the cell or the integrity of its various compartments. However there were several disadvantages on isotopic hybridization that led to the development of new techniques: 1) the nature of radioactive substances makes the probe unstable; 2) the resolution of the radiography is limited; 3) long exposure times (e.g. months) are often required to produce measurable signals (Carter et al. 2010), which contributes to the delay of the results and 4) radioactive labelled probes are a relatively costly and dangerous material and it requires to be transported, handled, stored and disposed according to specific regulations (Levsky & Singer 2003).

The first application of FISH was described in 1980, with a probe for a specific DNA sequence labelled with a fluorophore directly to the 3' end of RNA (Bauman et al. 1980). In 1989, DeLong used the first fluorescently-labelled oligodeoxynucleotides complementary to 16S rRNA for the detection of single microbial cells (DeLong et al. 1989). With the development of fluorescent labels, radioactive probes were steadily replaced by non-isotopic dyes (Pinkel et al. 1986; Pinkel et al. 1988). In comparison to radioactive probes, fluorescent probes allowed significant advances in speed and safety. Additionally, since fluorescent probes can be labelled with dyes of different emission wavelengths, FISH technique allows the detection

of multiple targets, within a single hybridization step in whole cells (Moter & Göbel 2000; Levsky & Singer 2003).

Different detection methods have been devised ever since, like chemiluminescent *in situ* hybridization (CISH) or enzyme-based chromogenic techniques (Hougaard et al. 1997). Thenceforth, although the number of detection methods has increased, the type of targets have become quite varied and the popularity of the assay led to a drastic increase in publications during the 1990s (Levsky & Singer 2003) (Fig. 2).

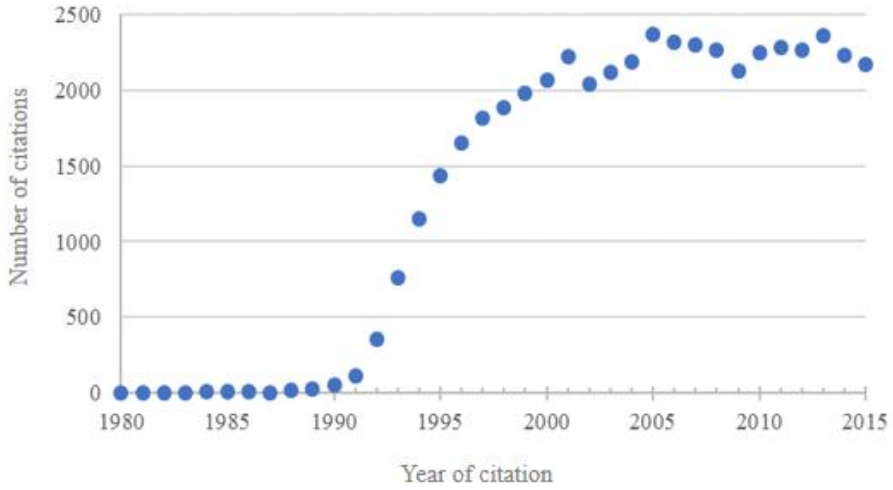

Figure 2. **Number of citations in the PubMed database for the keywords "fluorescence *in situ* hybridization" by year**, from 1980 to 2015. It can be observed that after the popularity of the assay during the 1990s, the number of publication has stabilized.

2.4.1. Fluorescence *in situ* Hybridization: Technical Aspects

2.4.1.1. Probe design

It is important to consider specificity and sensitivity when selecting a FISH-probe. As well as its ability to penetrate the outer cell layer. Specificity is theoretically expressed as a percentage, where the number of non-target strains that did not react with the probe is divided by the total number of non-target strains (Almeida et al. 2010). Specificity can be theoretically predicted through comparative sequence analysis and then implemented in the laboratory by optimising the hybridization and washing conditions (Hugenholtz et al. 2008). Sensitivity is expressed as a percentage where the number of microbial strains of interest detected by the probe is divided by the total number of strains of the microorganism of interest (Almeida et al. 2010). Short probes have an easier access to their target. A typical DNA oligonucleotide probe has between 18-30 base pairs (bp) (Wagner et al. 2003)..

There are different ways of labelling: “direct labelling” where the probe is labelled directly with the fluorophores by a chemical conjugation between the fluorophore and the acid probe and “indirect labelling” where the probe is capable of indirect association with fluorophores by chemical conjugation of the nucleic acid with a nonfluorescent molecule that can bind fluorescent material after hybridization (Fan

2003). Direct fluorescent labelling is more common because it is fastest, cheapest and easiest since it does not require detection steps after hybridization (Moter & Göbel 2000).

2.4.1.2. Protocol development

The FISH method involves five major steps: fixation, permeabilization, hybridization, washing and visualization (Fontenete et al. 2015; Cerqueira et al. 2008; Moter & Göbel 2000).

Usually fixation and permeabilization occur simultaneously with the objective to render the cell wall permeable to the oligonucleotide probe entry, while, simultaneously, assuring that cell lysis and nucleic acid probe degradation will not occur. The fixation step includes the application of chemical fixatives, such as formalin, paraformaldehyde and ethanol that are very commonly used in bacterial and human cells (Guimarães et al. 2007; Wagner et al. 2003).

During the hybridization step, the probe is placed in contact with the target cells, and if complementary (or near-complementary) sequences are present, hybridization will take place. Temperature, pH, formamide concentration and ionic strength need to be optimised in order to allow the probe to access to the target sequence and hybridisation to occur. The washing step ensures that loosely bound and unbound probes are removed from the sample, providing specificity to the method.

Probes used for FISH identification of Bacteria or Archaea usually target the 16S ribosomal RNA sequence, probes for Eukaryotes the 18S rRNA sequence. The rRNA is chosen as a target molecule due to its high abundance in the cell and consequently high fluorescence intensities are obtained as a result. Furthermore, rRNA is often used as a phylogenetic marker (Stender et al. 2002). The last step, visualization, can be carried out by either fluorescence microscopy or flow cytometry. This step allows the researcher to observe if the hybridization has occurred successfully (Fig. 3).

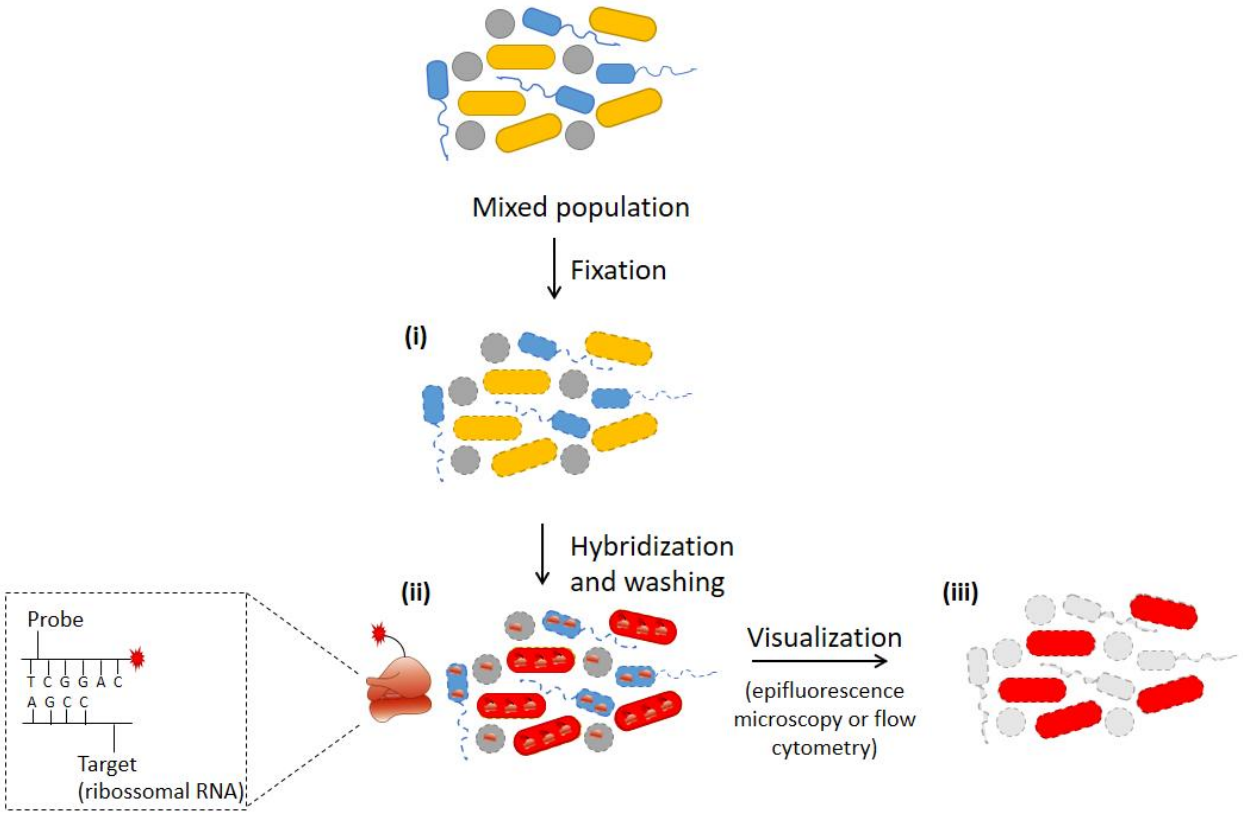

Figure 3. **Scheme of the fluorescence *in situ* hybridization method.** It is possible a mixed culture of bacteria, the probe only hybridizes with the target ribosomal RNA. The procedure includes the following steps: (i) fixation and preparation of the sample, that might include specific pre-treatment steps to render the cell wall permeable to the probe entry; (ii) hybridization of probes to the respective target sequences for detection; washing to remove unbound probes or loosely bound probes; (iii) visualization by epifluorescence microscopy or flow cytometry and documentation of the results.

2.4.2. Drawbacks

Although the application of FISH is recent, Cerqueira *et al*. (2008) assume that "all of those who have worked with this method are aware that not everything is straightforward in probe design and protocol development". This subchapter is focused on possible pitfalls, based on Moter and Göbel review (2000).

2.4.2.1. False Positive Results

Autofluorescence

One of the most striking problems in FISH is autofluorescence of microorganisms. This issue has been reported for a variety of fungi (Margo et al. 1967; Graham 1983) and for certain bacteria of the genus *Pseudomonas* (Brown & Lowbury 1965), *Legionella* (Wilkinson et al. 1990), *Rhodospirillum centenum* (Albrecht-Buehler 1997), for cyanobacteria (Schönhuber et al. 1999) and archaea (Hay Sørensen et al. 1997).

Lack of specificity

Reliability and accuracy of FISH is correlated with the specificity of the oligonucleotide probe. Critical evaluation of the probe design is essential. It is imperative to note that "an oligonucleotide is only as precise as the data from which it is derived" (Moter & Göbel 2000). Sequences from databases can contain errors (Bhatia et al. 1997) and the probe sequences should be checked using newest versions of sequencing data.

2.4.2.2. False negative results

Insufficient probe penetration

Low signal intensity may be the consequence of insufficient probe penetration. In the case of bacteria, it depends on the structure of the bacterial cell wall. Gram-positive bacteria may imply the need for pre-treatment with lysozymes or other proteolytic enzymes (Silverman & Kool 2007; Wagner et al. 1998; Moter & Göbel 2000). Gram-negative bacteria usually do not pose any problems as they are permeable to polyribonucleotide probes (Moter & Göbel 2000). Relatively to probe use in chytrids, its application recently unveiled that it may be problematic for lack of laboratory cultures which are necessary to test and validate its specificity and hybridization conditions of FISH probing (Jobard et al. 2010).

Higher order structure of target or probe

Due to the three-dimensional structure of the rRNA, not all sequences are equally accessible for probes. Loop and hairpin formation as well as rRNA-protein interactions obstructs hybridization and lead to differential signal intensity of oligonucleotide probes (Moter & Göbel 2000). For rRNA regions of difficult access, the hybridization time can be more than 96 hours (Yilmaz et al. 2006) which also contributes to the possibility of probe degradation by proteases or endonucleases (Yazbeck et al. 2002; Cummins et al. 1995).

Low rRNA content

Although the rRNA content is usually high it varies considerably, not only between species, but also within cells of one strain according to their metabolic and physiologic state (Stender et al. 2002; Pernthaler et al. 2002). Low physiological activity can result in low signal intensity and is directly correlated with their growth rate (DeLong et al. 1989; Kemp et al. 1993; Wallner et al. 1993; Poulsen et al. 1993).

Furthermore there have been concerns about the ability of the FISH method to discriminate between sequences with single-base mismatches, affecting the specificity (Shakeel et al. 2006). The reason why so many DNA probes fail to give intense signals has been recently related to low affinity between the probe

and the target. To increase affinity and boost the brightness of probes, the overall Gibbs free energy change (ΔG^o) should be negative and "below the threshold of 10-13.5 kcal/mol" (Yilmaz et al. 2006).

2.5. Nucleic Acid Mimics: Peptide Nucleic Acids (PNA)

The problems associated with DNA-FISH led to the development of alternative and improved methods, such as the use of nucleic acid analogues (Nielsen et al. 1991; Petersen et al. 2003), known as DNA mimics. In fact, the design and synthesis of peptide nucleic acids (PNA) (Nielsen et al. 1991), one of the first nucleic acid mimics, were only published two years after the description of the FISH technique by DeLong *et al*. (1989). Since then, the use of other nucleic acid analogues in FISH-applications has been rising exponentially (Cerqueira et al. 2008), including the use of PNA, locked nucleic acid (LNA) (Koshkin et al. 1998) and 2'-O-methyl (2'-OMe) RNA (Cummins et al. 1995).

PNA is a nucleobase oligomer in which the negatively charged backbone is replaced by a neutral backbone composed of N-(2-aminoethyl) glycine units (Nielsen et al. 1991; Corey et al. 1997; Nielsen & Egholm 1999; Egholm et al. 1992) (Fig. 4). Its structure allows hybridization with complementary DNA and RNA sequences. Chemical configuration, intramolecular distances and the configuration of the nucleobases are similar to the natural DNA and the position of nucleobases and their distance are identical to those in natural DNA (Nielsen 2001; Shakeel et al. 2006).

Unlike DNA, PNA does not contain any pentose sugar or phosphate groups that would confer to them a negative charge. Due to the nonpolar nature of PNA, the thermal stability is better in PNA/DNA duplexes compared to their DNA/DNA equivalents (Shakeel et al. 2006). This implies that the melting temperature (Tm) for PNA/DNA duplexes is higher than for corresponding DNA/DNA structure. The increased Tm allows the synthesis of shorter PNA probes. In fact, the optimal length for PNA probes is approximately 14-15 bp and while DNA probes have an optimal length between 18-30 bp (Wagner et al. 2003). Consequently, the effect on the Tm of a single-base mismatch in PNA/DNA hybridization will have a higher impact comparing to DNA/DNA hybridization.

The neutral peptide backbone of PNA also implies that the probe is chemically more stable and resistant to enzymatic hydrolysis, such as nucleases and proteases (Wagner et al. 2003; Stender et al. 2002; Demidov et al. 1994).

Furthermore, the neutral amide backbone of PNA supports hybridization with complementary DNA molecules under low-salt conditions. Positive ions are no longer needed to counteract between two negatively charged DNA-backbones (Shakeel et al. 2006; Nielsen 2001; Perry-O'Keefe et al. 2001). The absence of two repelling forces improves the hybridization, which in the end results in a better signal intensity.

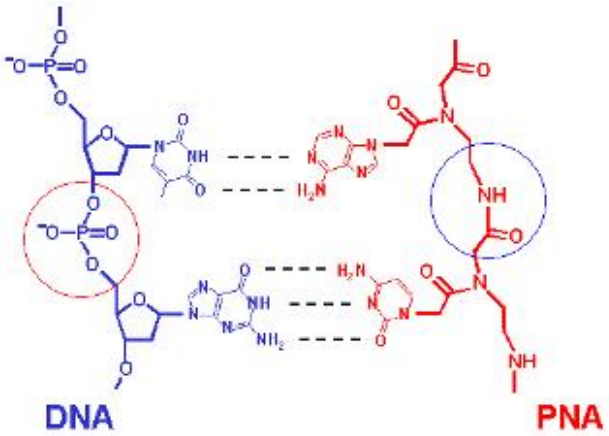

Figure 4. **Schematic representation of DNA and PNA chemical structure.** The negatively charged backbone of the DNA is replaced by a neutral backbone composed of glycine units. The PNA structure allows the hybridization with complementary DNA and RNA sequences. Reprinted with permission from Mateo-Mart & Pradier 2010.

In conclusion, PNA probes are very effective in FISH applications because of their neutral backbone, which provides a high specificity *in situ*, requires less concentration and hybridises faster. Additional advantages of using PNA probes *in situ* are reduced background binding, i.e. excellent signal-to-noise ratio, low photobleaching and a mild washing procedure (Shakeel et al. 2006).

Chapter 3

Materials and Methods

3.1. Culture maintenance

3.1.1. *Paraphysoderma sedebokerense* culture

The fungal strains PS1 and PS2 are both from outdoor cultures in Portugal. PS1 was isolated by Strittmatter and PS2 was isolated from Hiegle. PS1 and PS2 were maintained on Chytrid Growth Medium (CGM) (Appendix A1) at 25 ºC and, once *P. sedebokerense* takes 6-8 weeks to grow (Strittmatter et al. 2016), new cultures were streaked onto fresh plates once they were visible, to maintain them growing. The liquid cultures were incubated at 25 ºC on a shaker (Agitorb 200, Aralab) at 120 rpm and new cultures were prepared every three weeks.

3.1.2. *Haematococcus pluvialis* culture

H. pluvialis was cultivated according to Strittmatter et al. (2016) in Bold Basal Medium with 3-fold Nitrogen and Vitamins (3N-BBM+V) (Appendix A1) at 25 ºC in a 24h light period.

3.1.3. *Paraphysoderma*-infected *Haematococcus* cultures

The procedure for the *Paraphysoderma*-infected *Haematococcus* cultures was performed as described by Strittmatter et al. (2016). The primary infection was achieved by inoculating *H. pluvialis* in 3N-BBM+V medium with PS1 or PS2 strains from CGM agar. The infection was propagated by inoculating *H. pluvialis* with 5% (vol/vol) of infected culture. The progress of the infection and absence of eukaryotic contaminants in culture were monitored by optical observation with a light microscope.

3.2. *In silico* PNA probe design

The 18S rRNA gene sequences of *P. sedebokerense* available at the National Centre for Biotechnology Information (NCBI) website (https://www.ncbi.nlm.nih.gov/nuccore/) were used to design a probe. Two target sequences (KT270356.1 and KJ563218.1) with > 1200 bp in length were used to screen the entire 18S sequence. As control all available sequences (also with a minimum of 1200 bp) (https://www.ncbi.nlm.nih.gov/nuccore/) of the closest relatives, the *Physodermataceae*, were added to the dataset (HQ888719.1 and HQ888718.1 from *Urophlyctis pulposa*, HQ888717.1 from *Urophlyctis trifolii*, HQ888716.1 from *Physoderma lycopi* and lastly AY601708.1 from *Physoderma maydis*), as well as sequences of other organisms which might be present in the photobioreactor such as *H. pluvialis* (KC196725.1, KC196726.1, KM115647.1 and KT285940.1), *Chlorella vulgaris* (KJ148623.1,

KP341004.1, GQ122370.1, AY591515.1, KU720636.1) and *Scenedesmus sp.* (KT720478.1, KF879588.1, KC859922.2).

Sequences were aligned with Clustal Omega (http://www.ebi.ac.uk/Tools/msa/clustalo/) to select possible regions for probe design. This selection was based on regions that showed differences between the *P. sedebokerense* sequences to the non-target strains. Nucleotide BLAST (https://blast.ncbi.nlm.nih.gov/Blast.cgi) was used to test the potentially PNA probe oligonucleotide sequences, to screen for sequences with a higher number of *P. sedebokerense* sequences matches and lowest number of matches for non-target sequences. Besides sensitivity and specificity, the criteria for selection of the PNA probe sequence were the following:

- **Gibbs free energy** should be lower than -13 kcal/mol (Yilmaz *et. al* (2006));
- **Pyrimidine content** should be superior to 40%, since purine-rich PNA oligomers tend to aggregate and have low solubility in aqueous solutions;
- **Avoidance of self-complementary structures**, e.g. sequences with inverse repeats, hairpins and palindromes tend to aggregate as PNA/PNA interactions are stronger than PNA/DNA interactions;
- **Melting temperature** typically, 15 bp PNA will have a Tm of around 70 ºC. Both Tm and ΔG calculations were based on Fontenete *et al*. (2015).

The evaluation of self-complementary probes was performed with Applied Biosystems (http://www6.appliedbiosystems.com/support/pnadesigner.cfm).

The selection of the fluorophore was based on its excitation and emission gap and the availability of a suitable Fluorescence Microscope filter at A4F facilities. The selected probe sequence was ordered with a 5-FAM fluorophore (maximal excitation at 490 nm and maximal emission at 518 nm) attached, from Panagene, South Korea (http://www.panagene.com).

3.3. Theoretical evaluation of the PNA probe performance

The sensitivity of the probe was calculated based on the number of *P. sedebokerense* sequences that match with the probe divided by the total number of *P. sedebokerense* sequences. The probe sequence matches both available *P. sedebokerense* sequences therefore it is assumed that the sensitivity of the probe has the maximum value.

The formula used for the determination of the theoretical specificity (ts) was based on Almeida *et al.* (2010).

$$ts = \frac{nPs}{tPs} * 100$$

Where nPs stands for the number of non-*Paraphysoderma sedebokerense* strains that did not react with the probe and tPs is the total non-*Paraphysoderma sedebokerense* strains.

3.4. Hybridization procedure on glass slides

This procedure was the first to be tested, however, once the cells did not fix well and tend to be washed away the method was changed to the hybridization on suspension instead.

The hybridization protocol was performed as described by Guimarães *et al.* (2007) smears of each strain were prepared by standard procedures and immersed in 4% (wt/vol) of paraformaldehyde (Sigma) followed by 50% (vol/vol) ethanol for 15 minutes each and allowed to air dry. The smears were then covered with 30 µl of hybridization solution with 200 nM PNA probe containing 10% (wt/vol) dextran sulphate (Sigma), 10 mM NaCl (Sigma), 30% (vol/vol) formamide (Sigma), 0.1% (wt/vol) sodium pyrophosphate (Sigma), 0.2% (wt/vol) polyvinypyrrolidone (Sigma), 0.2% (wt/vol) Ficol (Sigma), 5 mM disodium EDTA (Sigma), 0.1% (vol/vol) Triton X-100 (Sigma), 50 mM Tris-HCl (pH 7.5, Sigma). Samples were covered with coverslips, placed in moist chambers, and incubated for 1h30min. Different hybridization temperatures, between 50 °C and 60 °C, were tested. Subsequently, the coverslips were removed, and the slides were submerged in a prewarmed washing solution containing 5 mM Tris base (Sigma), 15 mM NaCl (Sigma), and 1% (vol/vol) Triton X (pH 10; Sigma), and incubated for 30 min. Washing was performed at the hybridization temperature for 30 min, and then samples were dried at the incubator in the dark before being observed under the microscope.

3.5. Hybridization procedure on suspension

This procedure was based on Perry-O'Keefe et al. (2001) with slight modifications. 1 mL of liquid culture was pelleted by centrifugation at 15,700 *xg* for 5 min, resuspended in 400 µL of 4% (wt/vol) paraformaldehyde (Sigma), and fixed for 1 h at room temperature. The fixed cells were centrifuged at 15,700 *xg* for 5 min and resuspended in 500 µL of 50% (vol/vol) ethanol, and incubated for 30 min at -20 ºC. Subsequently, the fixed-cell aliquot was pelleted by centrifugation and resuspended in 200 µL of 0.05% (wt/vol) Sudan Black B in 70% (vol/vol) of ethanol, and incubated for 20 min at room temperature in the dark. Then, the samples were washed 3 times by centrifugation and resuspended in phosphate-buffer saline (PBS) containing 60 mM NaCl (Sigma), 1 mM KCl (ChemLab), 0.5 mM KH_2PO_4 (Sigma) and 9 mM $Na_2HPO_4 \cdot 2H_2O$ (Panreac). After that the cells were incubated with 100 µL of 200 nM PNA probe in hybridization solution containing (as described above) in the dark for 1 h. Different temperatures between 50 and 60 ºC were tested, the best results were obtained for 55 °C. After hybridization, cells were centrifuged at 15,700 *xg* for 5 min, resuspended in 200 µl of washing solution (as previously described), and incubated at 55 °C for 30 min. Washed suspension was pelleted by centrifugation and resuspended in 100 µl of PBS. Finally, 20 µl of the cell suspension was spread on a microscope slide to be observed under the microscope.

3.6. WGA-Rhodamine staining

The procedure for the wheat germ agglutinin (WGA)-Rhodamine staining was based on data from an unpublished study from Allewaert et al. (personal communication) with slight modifications. 1 mL of liquid culture was pelleted by centrifugation at 15,700 *xg* for 5 min, resuspended in 500 µL of 5 µg/mL WGA-Rhodamine which then incubated for 80 min at the dark. The suspension was then centrifuged at 15,700 *xg* for 5 min and washed two times with PBS. Finally, 20 µl of the cell suspension was spread on a microscope slide, covered with a coverslip and observed under the microscope.

3.7. Determination of the detection limit

To define the detection limit of *Paraphysoderma*-infected *Haematococcus* cultures, 30 mL of *Haematococcus* infected with PS1 and PS2, separately, were fixed with 4% (wt/vol) paraformaldehyde, followed by 50% (vol/vol) ethanol in a final volume of 15 mL (concentration of x2 factor), as mentioned above for the hybridization on suspension procedure. Then, 1 mL were used to the remaining steps of the FISH procedure and resuspended on the final volume of 100 µL (concentration of x10 factor).

The same was done to non-infected *Haematococcus* cells, which were fixed with 4% (wt/vol) paraformaldehyde, then by 50% (vol/vol) ethanol. The healthy (non-infected) *H. pluvialis* were then submitted to the remaining steps of the hybridization on suspension and then were used to dilute the *H. pluvialis* cultures infected with *P. sedebokerense* strains.

After the FISH procedure, PS-infected *H. pluvialis* cultures were diluted several times with healthy *Haematococcus* cultures. Additionally, were also done dilutions of the PS-infected *Haematococcus* cultures with water.

Then, using a haemocytometer the healthy and infected *H. pluvialis* cells were counted. *H. pluvialis* cells were considered infected if a *P. sedebokerense* was attached to their cell wall, independently if there were one or more *P. sedebokerense* cells attached. Only the *H. pluvialis* cells were counted.

The counting was performed in triplicate and the lowest number of total number of cells counted was 100. The percentage of infection was calculated based on the number of infected *H. pluvialis* cells divided by the total number of *H. pluvialis* cells. The number of infected cells counted [infected *H. pluvialis* cells/mL] was then converted to the original sample by applying the reverse dilution factors of 1:10 and 1:2, respectively.

3.8. Microscopy Analysis

The PNA probe has a 5-FAM fluorophore attached that can be monitored at excitation/emission wavelengths of 490/518 nm, respectively.

The hybridization on slides was only tested at FEUP, after the slides were dried, at the incubator in the dark, the smears were then mounted with one drop of nonfluorescent immersion oil (Merck). The samples were visualized using a Leica DM LB2 epifluorescence microscope. The microscope is equipped with one filter sensitive to the fluorophore, I3 (excitation, 450 to 490 nm; barrier, 510 nm; emission long-pass filter, 515 nm). The other filters are respectively N2.1 (excitation, 515 to 560 nm; barrier, 580 nm; emission long-pass filter, 590 nm); Y3 (excitation, 545/30 nm; barrier, 565; emission long-pass filter, 610/75) and A (excitation, 340 to 380 nm; barrier, 400 nm; emission long-pass filter, 425 nm). All images at FEUP were acquired using Leica Application Suite (LAS v4.2.) with a magnification of x1000.

The hybridization on suspension was tested in both facilities.

At A4F, the smears were covered with coverslips before observation under the Olympus BX3 microscope. The microscope is also equipped with one filter sensitive to the fluorophore, U-FBN filter (excitation, 470 to 495 nm; emission long-pass filter, 510 nm) (Fig. 5). The other filters are respectively U-FVN (excitation, 400 to 410 nm; emission long-pass filter, 460 nm) and U-FGNA (excitation, 540-550 nm; emission, 575 to 625 nm).

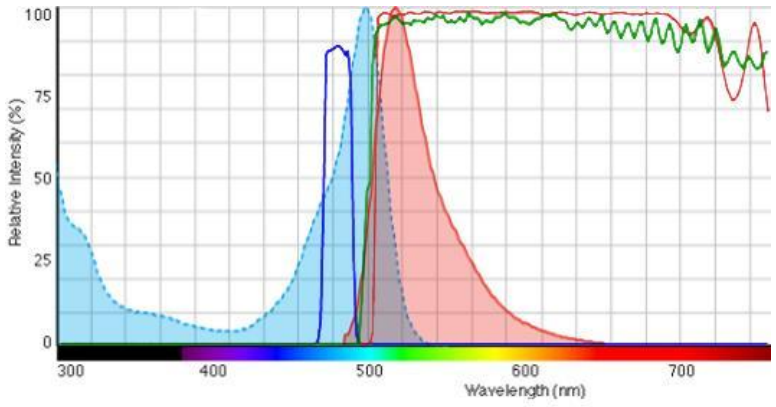

Figure 5. The relative transmittance intensity values of excitation filter (blue line) and emission filter (red line) of the U-FBN filter. The green line represents the dichromatic mirror. The excitation filter covers a range from 470 to 495 nm; the emission filter wavelength above 510 nm. Fluorescence spectra of the fluorophore 5-FAM, with a maximal excitation at 492 nm and maximal emission at 518 nm are represented by filled blue and red, respectively.

The WGA-Rhodamine procedure was only tested at A4F facilities. The cell suspension was covered with coverslips. Since Rhodamine was its maximum excitation and emission at 550/575 nm, the samples were observed under the U-FGNA fluorescence filter of the Olympus BX3 microscope.

3.9. Measurement of the intensity of fluorescence and statistics tests

To measure the intensity of fluorescence the Image J software (Wayne Rasband, National Institutes of Health) were used. The intensity of brightness was measured from several pictures for the temperatures between 50 and 60 ºC.

Then, to understand if there are significant differences between the different hybridization temperatures tested (50, 52, 54, 56, 58 and 60 ºC) an ANOVA test was applied. Also, to evaluate if there are significant differences between the use of the probe to the control samples (without the probe), the Student's *t* Test was applied to all tested temperatures. Both tests were done using SPSS (IBM Corporation).

Both ANOVA and Student's *t* Test are parametric statistics that can only be applied if there is normality. To evaluate the normality a Shapiro–Wilk test was used (Shapiro & Wilk 1965). The normality test of Shapiro ensures that there is normality when the significance is superior to 0.05. However, if the significance has a value inferior to 0.05, the values of skewness (Sk) and kurtosis (Ku) may be evaluated to overcome that condition. According to Kline (2011), if the Sk < 3 and Ku < 7, it can be considered that there are slight deviations from normality and parametric tests may still be applied.

For the ANOVA test, the sphericity was assessed using the Mauchly's Test of Sphericity, where again there is sphericity if the significance has a value superior to 0.05. If the significance was lower than 0.05, the corrector factor of Greenhouse Geisser for small samples (smaller than 30) can be applied.

The common statements about the significance values "$p < 0.05$", "$p > 0.05$" convey little information about the study's findings and rely on the convention of using 5% level of statistical significance to define two possible outcomes – significant or not significant. Rothman (1978) proposed the use of confidence levels, and during this thesis the significance is divided in four levels:

- $p > 0.05$ – not significant (NS)
- $0.05 \geq p < 0.01$ – significant (*)
- $0.01 \geq p < 0.001$ – very significant (**)
- $p \leq 0.001$ – extremely significant (***)

The significance levels were based on (Gardner & Altman 1986; Lunet et al. 2008).

Chapter 4

Results and discussion

4.1. Probe design

From the two regions of the 18S rRNA that showed differences for the non-target strains, sixteen sequences were analysed by the selection criteria (Gibbs free energy, pyrimidine content, avoidance of self-complementary structures and melting temperature) and only 8 sequences fulfil the desired characteristics for those parameters. The selected sequences were then assessed in terms of theoretical specificity and sensitivity. The selected probe has a theoretical specificity and sensitivity of 100%. All characteristics of the selected probe are represented below (Table 1).

Table 1. Characteristics of the selected probe and their values. The probe was designed for the detection of *P. sedebokerense*

Target sequence (5'-3')	GGGCTTGGTTGGGTG
Probe sequence (5'-3')	CACCCAACCAAGCCC
Number Base pairs	15
Sensitivity	100,00 %
Specificity	100,00 %
Melting temperature	82,94 ºC
Free Gibbs energy	-21,33 kcal/mol
Pyrimidine content	60,00 %
Complementary	Low

The theoretical melting temperature for the designed probe is 82.94 ºC. This is a bit higher than the optimal temperature according to the literature. However, the melting temperature decreases with the amount of formamide used (Moter & Göbel 2000). The pyrimidine content of the probe is 60 %, which is in agreement with several other probes found in the literature (Giesen et al. 1998; Sen & Nielsen 2006). The theoretical ΔG^o value is -21.33 kcal/mol, and it has been shown that the Free Gibbs energy should be below the threshold of -10 to -13.5 kcal/mol (Yilmaz & Noguera 2004; Yilmaz et al. 2006). A negative ΔG^o value is an indicator of a thermodynamically favourable reaction. Finally, the probe showed low self-complementarity, due to the absence of inverse repeats, hairpins and palindromes in the sequence.

4.2. Determination of theoretical specificity and sensitivity

The theoretical specificity and sensitivity of the probe were evaluated with the Nucleotide BLAST database. All matched sequences are listed in Appendix A2.

By applying the formula from Almeida *et al.* (2010) the theoretical specificity can be calculated. The number of total sequences present in the database is nearly 200 million (NCBI, December 2016). According to the Nucleotide BLAST the nPs is 198,565,414 and the tPs is 198,565,473, which gave a theoretical specificity of approximately 100%. The probe sequence matched a total of 63 sequences. However, of these, only two of the non-target sequences matched the rRNA and they are not morphologically similar to the organism of interest and are not known to be present in the photoreactors. All other matches belong to mRNA sequences or genomic sequences, which are less abundant in the cell and therefore would result in a lower fluorescence intensity even if hybridization occurred.

The probe sequence also matched the two target sequences of *P. sedebokerense*, which gives a theoretical sensitivity of 100%. The results for the probe sensitivity are highly related to the number of entire sequences available in the database.

4.3. Evaluation of autofluorescence and possible treatments

During protocol optimization, several issues were solved. One of the first problems faced was the inability to keep the cells on the slides during the FISH procedure, when using the hybridization on slides procedure. In fact, cells tended to be washed away with the addition of the solutions needed to perform the FISH method. Some adaptations were attempted, such as drying the sample using a flame instead of the incubator to improve the fixation of the cells to the slides. However, the cells kept unsticking and that issue was only overcome with the change of the protocol by doing the hybridization on suspension instead of hybridization on slides. Other problem faced was the autofluorescence of the organisms. Autofluorescence happens mostly due to the presence of cell endogenous fluorophores, such as chlorophyll in plants, and flavins, porphyrins and lipofuscin which are usually present in mitochondria and lysosomes in several cell types, as well as some extra-cellular matrix components such as collagen and elastin, and some exogenous dyes (Oliveira et al. 2010). For that reason, autofluorescence is not so common in FISH works regarding bacteria and is more usual in eukaryotic cells.

When assessing the experimental specificity, the probe was tested with *Saccharomyces cerevisae* and *H. pluvialis* as controls. The fluorescence intensity was measured with and without the probe, for both organisms. However, both organisms were autofluorescent in the green channel. The figures of the *Saccharomyces cerevisae* and *Haematococcus pluvialis* are presented below (Fig. 6).

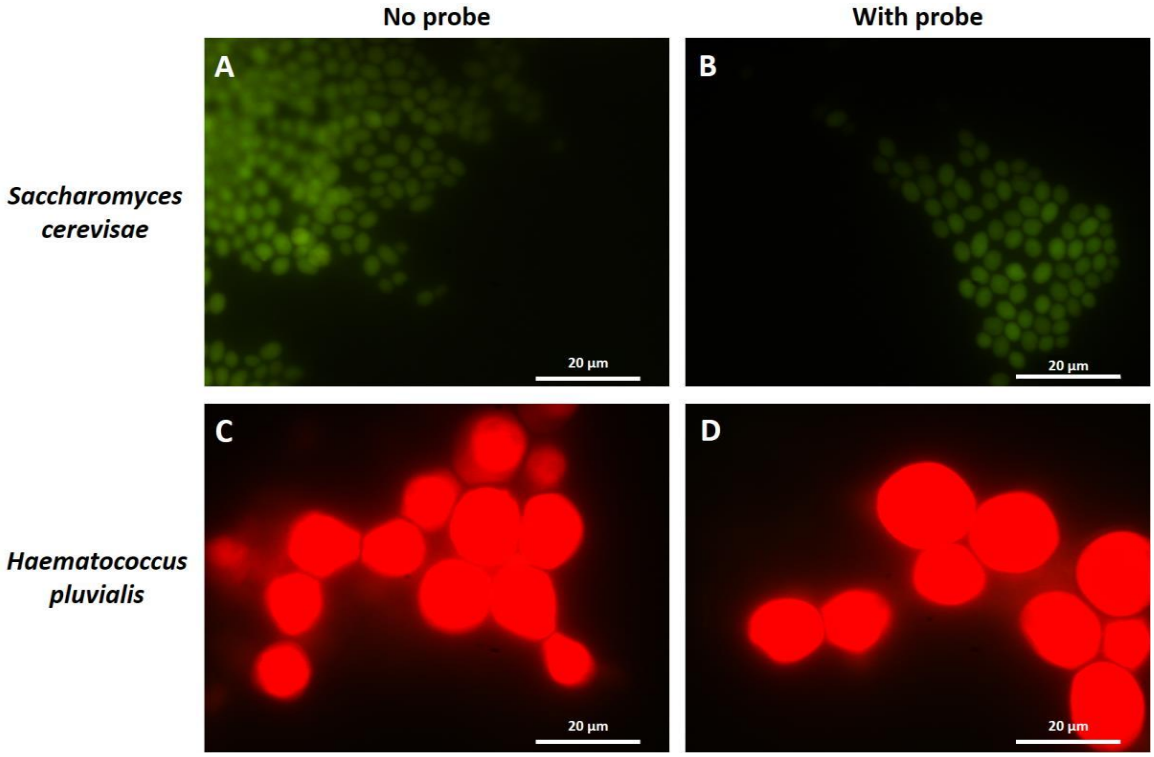

Figure 6. Specificity test for *Saccharomyces cerevisae* and *Haematococcus pluvialis*. *S. cerevisae* after the hybridization procedure on without the probe (A) and with the probe (B). *H. pluvialis* after the hybridization FISH without the probe (C) and with the probe (D). All images were acquired using Leica Application Suit (LAS v4.2) with a magnification of x1000 at I3 filter.

The graph representing the intensity of fluorescence in *Saccharomyces cerevisae* and *Haematococcus pluvialis* for the probe and control is presented below (Fig. 7). The fluorescence intensity was measured using Image J software. After ensuring the normality of the data, the *t* Test for both *Saccharomyces cerevisae* and *Haematococcus pluvialis* was applied and has showed non-significant differences between the use of the probe and the control ($p > 0.05$ for both microorganisms) (Appendix A3).

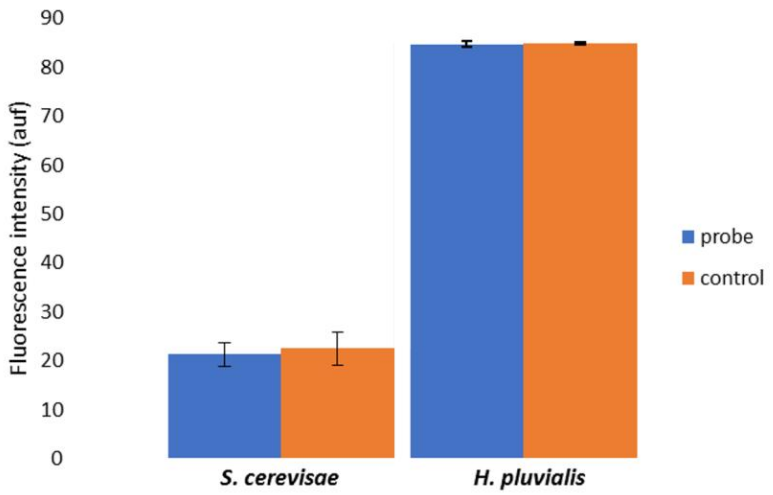

Figure 7. Intensity of fluorescence for *Haematococcus pluvialis* and *Saccharomyces cerevisae* with and without the probe. The temperature of hybridization was 57 ºC. All images were acquired using Leica Application Suite (LAS v4.2.) with a magnification of x1000 at I3 filter. Intensity of fluorescence was measure using ImageJ.

Even though it was only possible to test the specificity with two different organisms, due to the autofluorescence of both organisms it is not possible to infer that the probe did not react with them; or if the intensity of the probe was smaller in comparison with the autofluorescence of the organism and, for that reason, not detected. Which means that, although there were not significant differences ($p > 0.05$) observed when applying the *t* Test, those results are inconclusive.

This problem was also present with *P. sedebokerense* for which, due to its autofluorescence, differences when using the probe to the control could not be observed. To solve this issue, different procedures for autofluorescence reduction were tested. UV-irradiation was tested, as Neumann and Gabel (2002) reported that irradiating with visible or UV-light can reduce almost all autofluorescence. Photobleaching is a dynamic process where the light causes the cleavage of covalent bonds in fluorescent molecules, resulting in irreversible modifications that will eventually result in the loss of their ability to fluoresce (Song et al. 1995). However, the mechanisms of photobleaching in biological organisms are not yet well understood (Tsien et al. 2006) and it did not reduce the autofluorescence (Fig. 8).

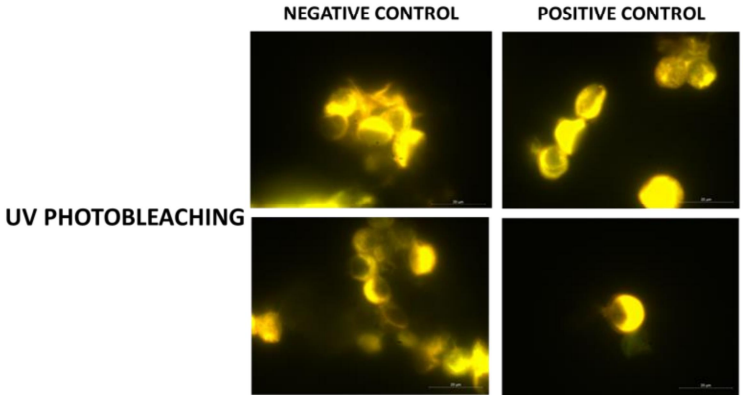

Figure 8. Images from FISH experiment on *Paraphysoderma sedebokerense* axenic culture after being subjected to 2h with UV radiation. Images acquired at the I3 filter using a x1000 magnification.

Also freezing at -80 ºC was tested, which has been widely reported to preserved the morphological structure of the organisms and maintained autofluorescence intensity at lowest levels (Demers et al. 1993; Harvey et al. 2009), this treatment also did not have positive results (Fig. 9).

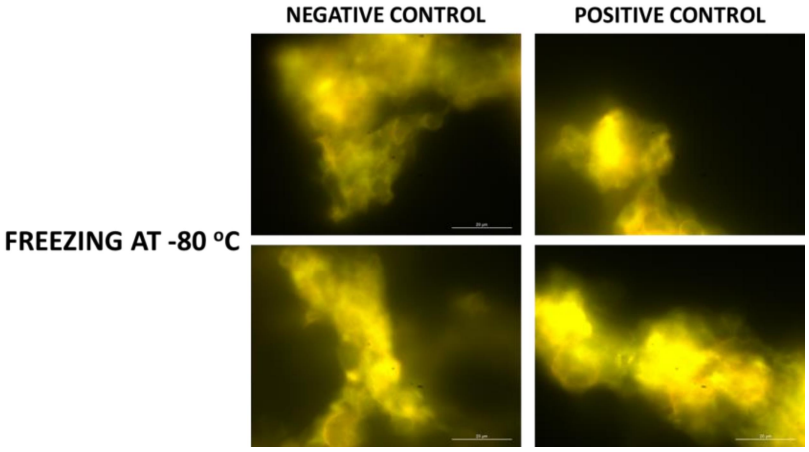

Figure 9. Images from FISH experiment on *Paraphysoderma sedebokerense* axenic culture after being subjected to an overnight freezing treatment at -80 ºC. Images acquired at the I3 filter using a x1000 magnification.

The use of Trypan Blue is also commonly reported on the literature (Busetto et al. 2004). Trypan blue is a quencher that absorbs the green fluorescence, upon binding to certain particles, causing them to fluorescence red instead (Loike & Silverstein 1983; Lipoglavsek & Avgustin 2001), results shown on the Figure 10. Additionally, it was tested the combination of UV photobleaching with Trypan Blue (Fig. 11).

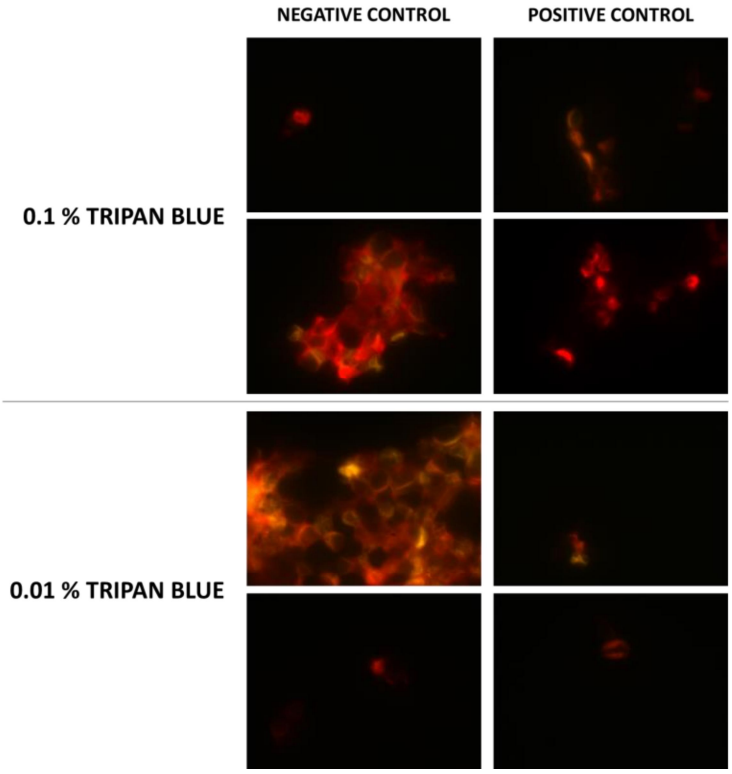

Figure 10. Images from FISH experiment on *Paraphysoderma sedebokerense* axenic culture after being treated with 0.1% and 0.01% Tripan Blue. Images acquired at the I3 filter using a x1000 magnification.

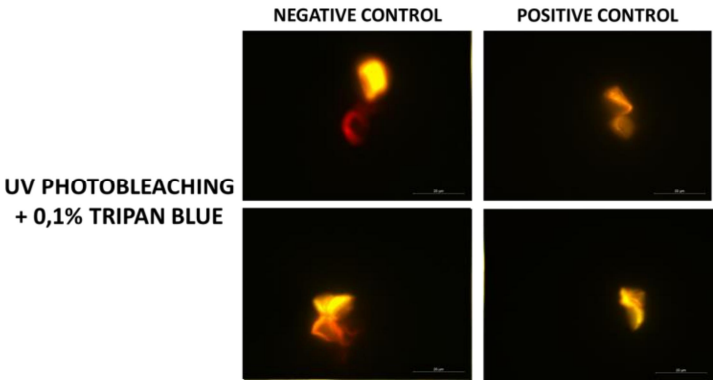

Figure 11. Images from FISH experiment on *Paraphysoderma sedebokerense* axenic culture after being subjected to 2h with UV radiation + 0.1% Tripan Blue. Images acquired at the I3 filter using a x1000 magnification.

Lastly, Sudan Black B, which is also frequently mentioned in the literature (Schnell et al. 1999; Neumann & Gabel 2002; Oliveira et al. 2010; Heaney et al. 2011), was also tested. Sudan Black B is mostly known for quenching the autofluorescence of lipids and some lipoproteins. However, Sudan Black B can be used to stain other substances, as it is not specific to lipids (Schnell et al. 1999). Of the autofluorescence reduction treatments mentioned above only the Sudan Black B showed positives results when reducing the autofluorescence of *P. sedebokerense* (Fig. 12).

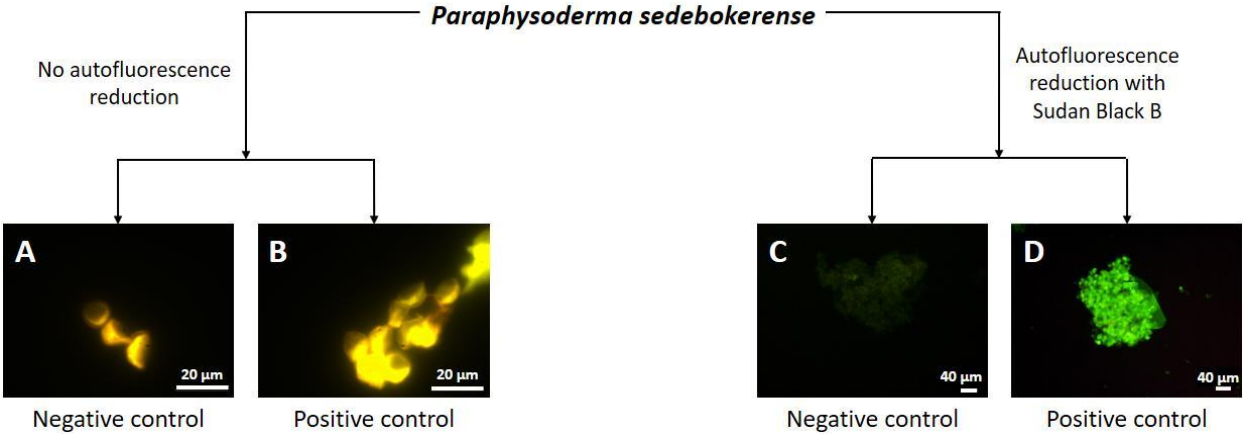

Figure 12. Compatibility of autofluorescence reduction treatment with Sudan Black B and fluorescence *in situ* hybridization using a PNA-probe. Axenic culture of PS1 without autofluorescence reduction after the hybridization procedure without the PNA-probe (A) and with the PNA-probe (B). Axenic culture of PS1 treated with 0.05% Sudan Black B (wt/vol) in 70% ethanol (vol/vol) for 20 min and after the hybridization protocol without the PNA-probe (C) and with the PNA-probe (D). Images A and B were acquired at FEUP with a magnification of x1000 using Leica Application Suite (LAS v4.2.) at the hybridization temperature of 57 ºC (filter I3). Images C and D were acquired at A4F using an Olympus BX3 microscope (filter U-FBN) at the hybridization temperature of 58 ºC with magnification of x200.

4.4. Determination of the hybridization temperature

Different hybridization temperatures, between 50 °C and 60 °C, were tested (50; 52; 54; 56; 58; 60). To evaluate which one is the most suitable temperature, two parametric statistics tests were implemented. Firstly, an analysis of variance (ANOVA) was implemented to the results using the probe to

compare the intensity of fluorescence for the different temperatures. From this test, it is possible to understand if there is any temperature where the intensity of fluorescence exceeds or is too low and may be eliminated. The other parametric test used was the Student's *t* Test, which was used to compare the intensity of fluorescence at same temperature, with and without the probe. To understand if there are significant differences when using the probe. All statistics were implemented using the SPSS software, additional information may be found at the Appendix A5.

As mentioned on the previous chapter, when parametric tests are used, it is important to ensure that all samples have a normal distribution. Hence, all probe samples were submitted to a normality evaluation using the Shapiro-Wilk test. The normality test of Shapiro ensures that there is normality when the significance is superior to 0.05. However, the significance was inferior to 0.05. To overcome that condition, the values of skewness (Sk) and kurtosis (Ku) were evaluated. According to Kline (2011), there are slight deviations from normality if the Sk < 3 and Ku < 7 and hence parametric tests can be applied. For every temperature tested, the values of skewness and kurtosis were inferior to 3 and 7, respectively, so the ANOVA test was employed.

Then, the sphericity of the samples was assessed using the Mauchly's Test of Sphericity. Because the significance was inferior to 0.05, the corrector factor of Greenhouse Geisser for small samples (inferior to 30) was applied and the sphericity was extremely significant, with a significance inferior to 0.001.

The results for the ANOVA test are expressed below (Table 2.).

Table 2. ANOVA test for the comparison between different temperatures of hybridization. Mean (μ), standard deviation (σ) and p values according to the Least Significant Difference (LSD)

	50	**52**	**54**	**56**	**58**	**60**
	μ = 17,486 σ = 2,953	μ = 32,214 σ = 3,873	μ = 36,707 σ = 4,084	μ = 37,013 σ = 3,023	μ = 29,955 σ = 3,328	μ = 21,848 σ = 2,490
50	-					
52	p = 0,000***	-				
54	p = 0,000***	p = 0,145	-			
56	p = 0,000***	p = 0,039*	p = 0,971	-		
58	p = 0,001***	p = 0,358	p = 0,041*	p = 0,001***	-	
60	p = 0,222	p = 0,001***	p = 0,000***	p = 0,000***	p = 0,009**	-

* - significant (p ≤0,05), ** - very significant (p ≤0,01), *** - extremely significant (p ≤0,001)

From Table 2. it is possible to observe some extremely significant differences. For the temperature of 50 ºC, extremely significant differences were detected for the temperatures from 52 to 58 ºC. Considering the average value for 50 ºC it is possible to conclude that it is lower than the remaining temperatures,

justifying the extremely significant differences observed. The same is observed for the temperature of 60 ºC, where extremely significant and very significant differences were detected for the temperatures on the rage between 52 and 58 ºC, again acceptable due to the lower mean value observed when compared to the other temperatures. An extremely significant difference between 56 and 58 ºC, and a significant difference between 52 and 56 ºC, and between 54 and 58 ºC was also observed.

To evaluate if there is a statistically significant difference between the use of the probe and the control, six *t* Student tests were done for the different temperatures. Again, to use a parametric test it is required to ensure that there is normality in the samples. Since the normality was already tested for the samples using the probe, it was done for the control samples for the different temperatures using the Shapiro-Wilk test. The normality test gave a significance superior to 0.05 for the control samples at 56 and 58 ºC, the remaining temperatures had a significance inferior to 0.05. For those temperatures, the Kline theory was adopted and since the skewness and the kurtosis value were inferior to 3 and 7, respectively, it is still possible to use the *t* Test. The Figure 9 represents the intensity of fluorescence for the different temperatures and the results acquired from the *t* Test. It is possible to observe an extremely significant difference between the samples treated with and without the probe. Which proves that despite the temperature chosen between 50 to 60 ºC, there is a clear difference noted from the effect of the probe.

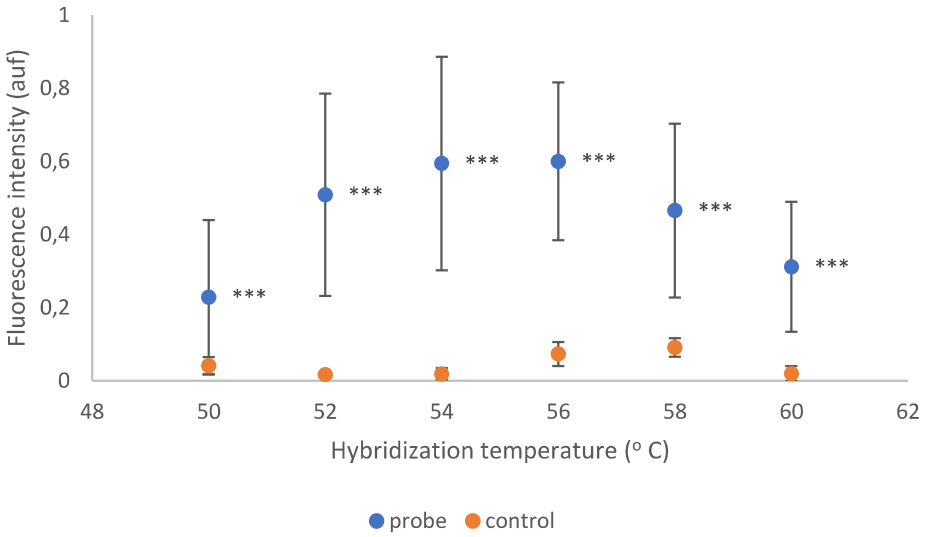

Figure 13. Intensity of fluorescence normalized for temperatures between 50 and 60 ºC, with and without the probe (blue and orange, respectively). The results obtained are from three independent FISH experiments. The *** represent an extremely significant difference ($p < 0.001$) between the collected data for the same temperature, with and without the probe.

From the statistics tests applied and analysing the results obtained it is possible to conclude that the optimal temperature of hybridization should be between 54 and 56 ºC, because both have significant differences to other temperatures, a higher average and an extremely significant difference to the same sample treated without the probe. It is possible to observe that the fluorescence intensity tends to increase until 54 ºC and then decreases. This behaviour is justified as the increase of temperature initially speed up

the process by creating the necessary "disorder of the chemical components" (entropy), contributing for the probe hybridization. For temperatures above 56 ºC the entropy leads to the disruption of the hydrogen bounds between the paired bases of the probe and the target sequence, which has a negative effect for the stability of the molecules (Lehninger 1871). In the end, 55 ºC was selected as the optimal hybridization temperature.

4.5. WGA-Rhodamine staining

To ensure the validation of the FISH method, other technique was used to detect *P. sedebokerense* to compare the results obtained in mixed cultures. Wheat germ agglutinin (WGA) is a lectin present in wheat (*Triticum vulgaris*). Lectins are carbohydrate-binding proteins that are highly specific for sugar moieties. WGA protects the wheat from insects, yeast and bacteria. This lectin has a primary specificity to N-acetyl-D-glucosamine which is the main component of chitin, present on the cell wall of the chytrids. It has been reported to bind *P. sedebokerense* zoospores and cysts without interfering with *Haematococcus* cells (Gutman et al. 2011).

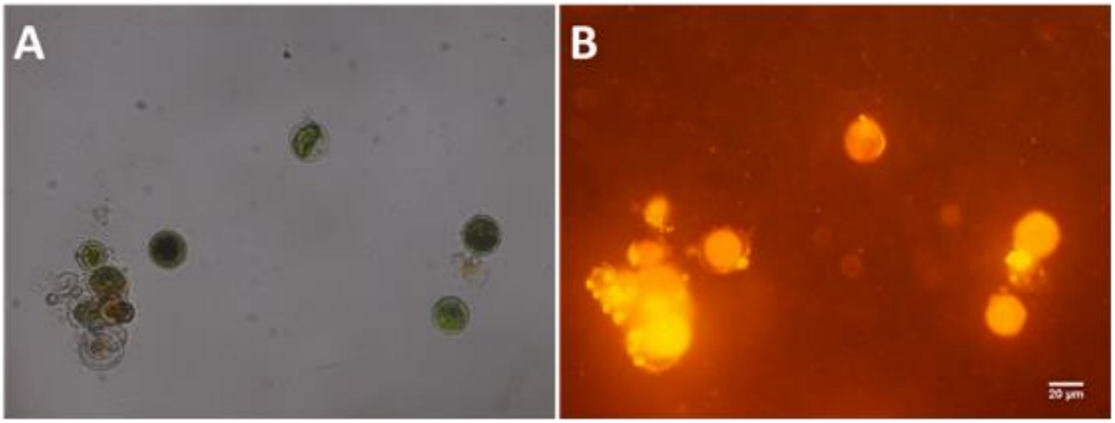

Figure 84. WGA-Rhodamine staining at *Haematococcus* infected by *Paraphysoderma sedebokerense*. A – bright field, B – U FGNA filter. Magnification of x400.

This procedure, when compared to FISH, is faster. Yet, sometimes positive results were observed that could not be proved using the bright field. It might be a small, non-visible zoospore or bacteria. The mixed cultures used were not axenic and WGA also binds to sugar moieties present on bacteria cell wall. The lack of specificity of the WGA might, similarly to Calcofluor white, lead to false positive results.

Although the WGA-Rhodamine has such a bright orange colour, it is easier to observe a contrast of the green 5-FAM fluorophore with the remaining red autofluorescence of the *H. pluvialis*. This means that with the naked eye it is easier to distinguish the green 5-FAM fluorophore in the *P. sedebokerense* cells from the red *H. pluvialis*, then the orange from the Rhodamine in the *P. sedebokerense* cells from the red *H. pluvialis* cells.

4.6. Determination of the detection limits

When applying the FISH procedure with mixed cultures of *P. sedebokerense* with *H. pluvialis*, one of the goals was to determine the limit of detection. To do so, infected *H. pluvialis* with PS1 strain were diluted with healthy (non-infected) *H. pluvialis* cells. During the process of counting, healthy and infected *Haematococcus* cells were counted. *H. pluvialis* cells were considered infected if *P. sedebokerense* cells were encysted at *H. pluvialis* surface, no matter how many cells were attached (Fig. 11.).

Other dilutions of *H. pluvialis* infected with PS1 diluted with water; *H. pluvialis* infected with PS2 diluted with water, and diluted with healthy *Haematococcus* were out of the limit of quantification (the total number of cells counted were inferior to 100 cells). The results from those firsts experiments are on Appendix A6. Still, the results obtained from those experiments agree with the results shown in this section.

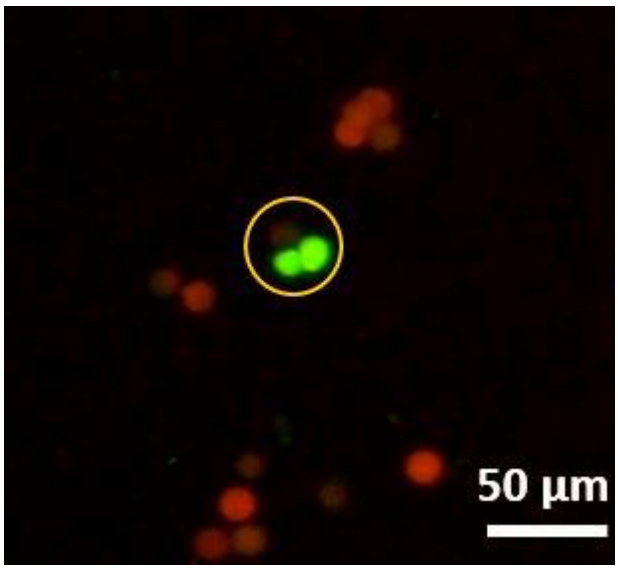

Figure 95. Example of a *H. pluvialis* infected cell by two *P. sedebokerense*. This image was obtained using the fluorescence U-FBN filter. Original magnification of x1000.

The initial number of *H. pluvialis* cells was 5.1 x 10^5 cells/mL, and the initial total number of infected cells was 2.1 x 10^5 cells/mL. From that initial solution, several dilutions were done with healthy *H. pluvialis*. The results obtained from the counting are expressed on Figure 12, where the percentage of infection (infected *H. pluvialis* cells divided by the total number of *H. pluvialis* cells), according to the different dilution series are represented. By calculating the x value for the intersection of the calibration curve for a y = 0 it is acquired the dilution where the percentage of infection equals to zero. Multiplying that dilution by the total number of infected cells it is possible to estimate the detection limit for the concentrated sample which is visualized at the haemocytometer. Subsequently, by applying the dilution factor of 1:20, the detection limit for the infected *Haematococcus* cells for the original retrieved sample can be estimated.

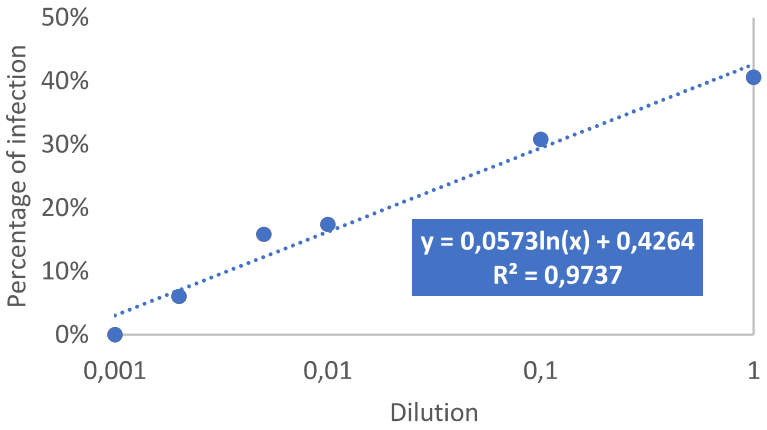

Figure 106. Percentage of infection (infected *H. pluvialis* cells with *P. sedebokerense* (PS1 strain), divided by the total number of *H. pluvialis* cells) versus a dilution factor of PS1-infected *Haematococcus* with healthy *Haematococcus*.

The detection limit for the concentrated sample is acquired by applying the described calculation. This value represents the number of cells visible at the haemocytometer which was 121 *H. pluvialis* infected cells/mL. Then, dividing per 20 (by applying the dilutions factors used of 1:2 and 1:10, respectively), a detection limit for the original sample can be predicted. The detection limit for the original sample is 6 cells/mL. Although some of the points for the highest dilutions were out of the quantification limit, from the remaining experiments, the result of those trials lead to a detection limit of 6 ± 4 cells/mL. Those results may be found on Appendix A6.

There were also some complications regarding the difficulty to homogenize the solutions. *Haematococcus* cells tend to form clumps that might hamper the counting process. To solve this issue, beside pipetting several times with different size tips, a syringe was used to resuspend the solution before placing at the haemocytometer.

Although for the detection limit only *H. pluvialis* cells were counted. It is also possible to observe *P. sedebokerense* not yet attached to *H. pluvialis* cells, which allows an early stage detection (Fig. 13).

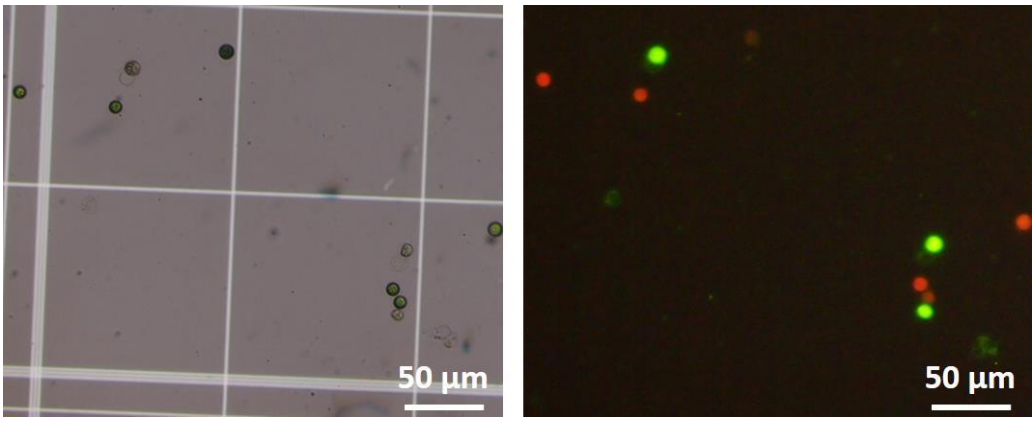

Figure 17. *Paraphysoderma*-infected *H. pluvialis* culture. At left, image acquired at bright field. At right, image acquired using the U-FBN filter. It is possible to observe the *P. sedebokerense* attached and unattached to *H. pluvialis* cells. Original magnification of x100.

Chapter 5

Concluding remarks and future work

5.1. General conclusions

During this thesis, a probe to detect the fungal parasite *P. sedebokerense* was designed *in silico* and after synthesis and protocol optimization was successfully applied in mixed cultures. The designed probe fulfils the selection criteria and has proved to have a high sensitivity to the *P. sedebokerense*, confirmed from the affinity of the probe to both, PS1 and PS2 strains. Although the specificity was not tested for a substantial number of other microorganisms, the probe also demonstrated a high specificity using *in silico* databases. During the test with mixed cultures, the green signal from *Paraphysoderma* differs a lot from the red autofluorescence from *Haematococcus* cells and is easily detectable.

Throughout the optimization procedure, several complications were overcome, such as: the difficulty to maintain the PS culture during the hybridization on slides, which were surpassed by the change of procedure to a hybridization on suspension; and also the strong autofluorescence signal from the parasite that could not be removed from several reduction treatments quoted on the literature (e.g. Trypan Blue, UV photobleaching, freezing at -80 ºC), being only overcome by the use of Sudan Black B.

After overcoming those difficulties, it was possible to optimize the FISH method. An extremely statistical significant difference ($p < 0.001$) between the use of the probe to the control sample was observed, at least among the range of hybridization temperatures tested between 50 to 60 ºC. According to the statistics tests applied, the most suitable temperature for the hybridization should be near 54 and 56 ºC, due to a higher average value compared to the other hybridization temperatures tested and significant differences observed at the ANOVA test.

FISH was proved to be a rapid technique for the screening of contaminants since it is possible to provide results, during a working day, while other molecular detection methods based on plating assays that can take up to three days to provide results. An early detection of parasites is essential to ensure the efficacy of possible infection treatments and to reduce possible costs. Also, due to the specificity of this technique it is possible to observe *P. sedebokerense* in its amoeboid and encysted form.

In contrast to the traditional detection methods, FISH allows the *in situ* detection, permitting a visualization of the culture in its actual form. Since it is possible to visualize chytrids not attached yet to the cells it allows the detection of the infection at an early stage.

Staining methods such as the use of Calcofluor White or WGA-Rhodamine may be quicker detection methods, however it is important to be aware of possible false positives. Yet, WGA-Rhodamine may be preferable once it does not stain the *H. pluvialis* cells, unlike Calcofluor White.

5.2. Future work

Control of parasites remains to be the primary concern for *Haematococcus* growers, as it remains the major issue for astaxanthin productivity and culture stability. As the method was successfully applied at the laboratory facilities, eventually it should be important to test this procedure for outdoor *Haematococcus* cultures at pilot-scale.

Due to the high specificity of the FISH method, and also its speed in providing results, it should be analysed the need to develop new probes for the detection of other prejudicial contaminants. One particular case would be for the detection of *Vibrio spp.* which are particularly problematic in *Nannochloropsis spp.* cultures. Some assays were already done with PNA-probes for *Vibrio spp.* detection in *Nannochloropsis spp.* cultures, yet, they still need protocol development and improvement. For that reason, those results are not mentioned on this thesis.

It would also be interesting to analyse the possibility to evaluate the FISH results by flow cytometry, instead of epifluorescence microscopy which may be less time consuming, as it could provide a faster analysis of a larger number of cells.

Bibliography

Albrecht-Buehler, G., 1997. Autofluorescence of Live Purple Bacteria in the Near Infrared. *Experimental Cell Research*, 236(1), pp.43–50.

Allewaert, C. et al., *Susceptibility of the blood algae Haematococcus to infection by the pathogen Paraphysoderma sedebokerense (Blastocladiomycota) is genetically and morphologically determined*,

Almeida, C. et al., 2010. Fluorescence in situ hybridization method using a peptide nucleic acid probe for identification of salmonella spp. in a broad spectrum of samples. *Applied and Environmental Microbiology*, 76(13), pp.4476–4485.

Amann, R.I., Krumholz, L. & Stahl, D.A., 1990. Fluorescent-oligonucleotide probing of whole cells for determinative, phylogenetic, and environmental studies in microbiology. *Journal of Bacteriology*, 172(2), pp.762–770.

Amann, R.I., Ludwig, W. & Schleifer, K.H., 1995. Phylogenetic identification and in situ detection of individual microbial cells without cultivation . Phylogenetic Identification and In Situ Detection of Individual Microbial Cells without Cultivation. *Microbiological reviews*, 59(1), pp.143–169. Available at: http://mmbr.asm.org/content/59/1/143.short.

Bauman, J.G. et al., 1980. A new method for fluorescence microscopical localization of specific DNA sequences by in situ hybridization of fluorochromelabelled RNA. *Experimental cell research*, 128(2), pp.485–90. Available at: http://www.ncbi.nlm.nih.gov/pubmed/6157553.

Bhatia, U., Robison, K. & Gilbert, W., 1997. Dealing with Database Explosion: A Cautionary Note. *Science*, 276(5319).

Borowitzka, M.A., 2013. High-value products from microalgae—their development and commercialisation. *Journal of Applied Phycology*, 25(3), pp.743–756. Available at: http://link.springer.com/10.1007/s10811-013-9983-9.

Botes, M., de Kwaadsteniet, M. & Cloete, T.E., 2013. Application of quantitative PCR for the detection of microorganisms in water. *Analytical and Bioanalytical Chemistry*, 405(1), pp.91–108. Available at: http://link.springer.com/10.1007/s00216-012-6399-3.

Boussiba, S., 2000. Carotenogenesis in the green alga Haematococcus pluvialis: Cellular physiology and stress response. *Physiologia Plantarum*, 108(2), pp.111–117. Available at: http://doi.wiley.com/10.1034/j.1399-3054.2000.108002111.x.

Boussiba, S. & Vonshak, A., 1991. Astaxanthin Accumulation in the Green Alga Haematococcus pluvialis1. *Plant and Cell Physiology*, 32(7), pp.1077–1082. Available at: https://academic.oup.com/pcp/article/1923449/Astaxanthin.

Brennan, L. & Owende, P., 2009. Biofuels from microalgae - A review of technologies for production, processing, and extractions of biofuels and co-products. *Renewable and Sustainable Energy Reviews*.

Brown, V.I. & Lowbury, E.J.L., 1965. Use of an improved cetrimide agar medium and other culture methods for Pseudomonas aeruginosa. *J. clin. Path*, 18, pp.752–756.

Busetto, S. et al., 2004. A single-step, sensitive flow cytofluorometric assay for the simultaneous assessment of membrane-bound and ingestedCandida albicans in phagocytosing neutrophils. *Cytometry*, 58A(2), pp.201–206. Available at: http://www.ncbi.nlm.nih.gov/pubmed/15057974.

Buskey, E.J. & Hyatt, C.J., 2006. Use of the FlowCAM for semi-automated recognition and enumeration of red tide cells (Karenia brevis) in natural plankton samples. *Harmful Algae*, 5(6), pp.685–692.

Del Campo, J.A. et al., 2004. Accumulation of astaxanthin and lutein in Chlorella zofingiensis (Chlorophyta). *Applied Microbiology and Biotechnology*, 64(6), pp.848–854. Available at: http://link.springer.com/10.1007/s00253-003-1510-5.

Del Campo, J.A., García-González, M. & Guerrero, M.G., 2007. Outdoor cultivation of microalgae for carotenoid production: current state and perspectives. *Appl Microbiol Biotechnol*, 74, p.1163.

Canter, H.M. & Jaworsky, G.H.M., 1980. Some general observations on zoospores of chytrid thizophydium planktonicum carter emend. *New Phytologist*, 84(3), pp.515–531. Available at: http://doi.wiley.com/10.1111/j.1469-8137.1980.tb04559.x.

Capelli, B., Jenkins, U. & Cysewski, G.R., 2013. Chapter 48 – Role of Astaxanthin in Sports Nutrition. In *Nutrition and Enhanced Sports Performance*. pp. 465–471.

Cardozo, K.H.M. et al., 2006. Metabolites from algae with economical impact.

Carney, L.T. et al., 2014. Microbiome analysis of a microalgal mass culture growing in municipal wastewater in a prototype OMEGA photobioreactor. *Algal Research*, 4, pp.52–61.

Carney, L.T. & Lane, T.W., 2014. Parasites in algae mass culture. *Frontiers in microbiology*, 5, p.278. Available at: http://www.ncbi.nlm.nih.gov/pubmed/24936200.

Carter, B.S., Fletcher, J.S. & Thompson, R.C., 2010. Analysis of messenger RNA expression by in situ hybridization using RNA probes synthesized via in vitro transcription. *Methods (San Diego, Calif.)*, 52(4), pp.322–31. Available at: http://www.ncbi.nlm.nih.gov/pubmed/20699122.

Cerqueira, L. et al., 2008. DNA mimics for the rapid identification of microorganisms by fluorescence in situ hybridization (FISH). *International Journal of Molecular Sciences*, 9(10), pp.1944–1960.

Chen, Z. et al., 2014. First report of Pseudobodo sp, a new pathogen for a potential energy-producing algae: Chlorella vulgaris cultures. *PloS one*, 9(3), p.e89571. Available at: http://www.ncbi.nlm.nih.gov/pubmed/24599263.

Chiaramonti, D. et al., 2015. Life Cycle Assessment of Algae Biofuels: Needs and challenges. *Applied Energy*, 154(September).

Chisti, Y., 2007. Biodiesel from microalgae. *Biotechnology Advances*, 25, pp.294–306.

Corey, D.R. et al., 1997. Peptide nucleic acids: expanding the scope of nucleic acid recognition. *Trends in biotechnology*, 15(6), pp.224–9. Available at: http://www.ncbi.nlm.nih.gov/pubmed/9183865.

Cummins, L.L. et al., 1995. Characterization of fully 2'-modified oligoribonucleotide hetero-and homoduplex hybridization andnuclease sensitivity. *Nucleic Acids Research*, 23(11), pp.2019–2024.

Damiani, M.C. et al., 2006. Ultrastructure of the cyst wall of Haematococcus pluvialis (Chlorophyceae): wall development and behaviour during cyst germination. *Phycologia*, 45(6), pp.616–623. Available at: http://www.phycologia.org/doi/abs/10.2216/05-27.1.

Day, J.G. et al., 2012. *Early detection of protozoan grazers in algal biofuel cultures*,

DeLong, E., Wickham, G. & Pace, N., 1989. Phylogenetic stains: ribosomal RNA-based probes for the identification of single cells. *Science*, 243(4896).

Demers, A. et al., 1993. Immunofluorescence identification of early life history stages of scallops (Pectinidae). *Marine Ecology Progress Series*, 97(1), pp.83–89.

Demidov, V. V et al., 1994. Stability of peptide nucleic acids in human serum and cellular extracts. *Biochemical pharmacology*, 48(6), pp.1310–3. Available at: http://www.ncbi.nlm.nih.gov/pubmed/7945427.

Egholm, M. et al., 1992. Peptide nucleic acids (PNA). Oligonucleotide analogs with an achiral peptide backbone. *Journal of the American Chemical Society*, 114(5), pp.1895–1897. Available at: http://pubs.acs.org/doi/abs/10.1021/ja00031a062.

Fan, L., Vonshak, A. & Boussiba, S., 1994. Effect of temperature and irradiance on growth of Haematococcus pluvialis (Chlorophyceae). *Journal of Phycology*, 30(5), pp.829–833.

Fan, Y.-S., 2003. *Molecular Cytogenetics: Protocols and Applications*,

Fontenete, S. et al., 2015. Prediction of melting temperatures in fluorescence in situ hybridization (FISH) procedures using thermodynamic models. *Critical Reviews in Biotechnology*, 8551(December), pp.1–12.

Gardner, M.J. & Altman, D.G., 1986. Statistics in Medicine Confidence intervals rather than P values: estimation rather than hypothesis testing. *British Medical Journal*, 292, pp.746–750. Available at: https://www.ncbi.nlm.nih.gov/pmc/articles/PMC1339793/pdf/bmjcred00225-0036.pdf.

Giesen, U. et al., 1998. A formula for thermal stability (Tm) prediction of PNA/DNA duplexes. *Nucleic Acids Research*, 26(21), pp.5004–5006. Available at: https://www.ncbi.nlm.nih.gov/pmc/articles/PMC147916/pdf/265004.pdf.

Graham, A.R., 1983. Fungal Autofluorescence with Ultraviolet Illumination. *Am J Clin Pathol*, 79, pp.231–234.

Gromov, B. V, Plujusch, A. V & Mamkaeva, K.A., 1999. Morphology and possible host range of Rhizophydium algavorum sp. nov. (Chytridiales) -an obligate parasite of algae. *Protistology*, 1(2), pp.62–65.

Guimarães, N. et al., 2007. Development and application of a novel peptide nucleic acid probe for the specific detection of Helicobacter pylori in gastric biopsy specimens. *Journal of Clinical Microbiology*, 45(9), pp.3089–3094.

Gutman, J., Zarka, A. & Boussiba, S., 2011. Evidence for the involvement of surface carbohydrates in the recognition of Haematococcus pluvialis by parasitic blastoclad Paraphysoderma sedebokerensis. *Fungal B*, 115, pp.803–811.

Gutman, J., Zarka, A. & Boussiba, S., 2009. The host-range of Paraphysoderma sedebokerensis, a chytrid that infects Haematococcus pluvialis. *European Journal of Phycology*, 44(4), pp.509–514. Available at: http://www.tandfonline.com/doi/abs/10.1080/09670260903161024.

Han, D., Li, Y. & Hu, Q., 2013. Biology and Commercial Aspects of Haematococcus pluvialis. In *Handbook of Microalgal Culture*. Oxford, UK: John Wiley & Sons, Ltd, pp. 388–405. Available at: http://doi.wiley.com/10.1002/9781118567166.ch20.

Harvey, J.B.J., Hoy, M.S. & Rodriguez, R.J., 2009. Molecular detection of native and invasive marine invertebrate larvae present in ballast and open water environmental samples collected in Puget Sound. *Journal of Experimental Marine Biology and Ecology*, 369(2), pp.93–99. Available at: http://dx.doi.org/10.1016/j.jembe.2008.10.030.

Havlik, I. et al., 2013. Monitoring of microalgal cultivations with on-line, flow-through microscopy. *Algal Research*, 2(3), pp.253–257. Available at: http://linkinghub.elsevier.com/retrieve/pii/S2211926413000489.

Hay Sørensen, A. et al., 1997. Whole-Cell Hybridization of Methanosarcina Cells with Two New Oligonucleotide Probes. *Applied and Environmental Microbiology*, 63(8), pp.3043–3050.

Heaney, S. a., Maloy, a. P. & Slater, J.W., 2011. Evaluation of fixatives and autofluorescence reduction treatments for marine bivalve larvae. *Journal of the Marine Biological Association of the United Kingdom*, 91(7), pp.1567–1576. Available at: http://www.journals.cambridge.org/abstract_S0025315411000208.

Hoffman, Y. et al., 2008. Isolation and characterization of a novel chytrid species (phylum Blastocladiomycota), parasitic on the green alga Haematococcus. *Mycological Research*, 112(1), pp.70–81. Available at: http://www.ncbi.nlm.nih.gov/pubmed/18222678.

Hougaard, D.M., Hansen, H. & Larsson, L.-I., 1997. Non-radioactive in situ hybridization for mRNA with emphasis on the use of oligodeoxynucleotide probes. *Histochemistry and Cell Biology*, 108(4–5), pp.335–344. Available at: http://link.springer.com/10.1007/s004180050174.

Hugenholtz, P., Tyson, G.W. & Blackall, L.L., 2008. Design and Evaluation of 16S rRNA-Targeted Oligonucleotide Probes for Fluorescence In Situ Hybridization. In *Gene Probes*. New Jersey: Humana Press, pp. 29–42. Available at: http://link.springer.com/10.1385/1-59259-238-4:029.

Ibañez, E. & Cifuentes, A., 2013. Benefits of using algae as natural sources of functional ingredients. *Journal of the Science of Food and Agriculture*, 93(4), pp.703–709. Available at: http://doi.wiley.com/10.1002/jsfa.6023.

James, T.Y. et al., 2011. Paraphysoderma sedebokerense, gen. et sp. nov., an aplanosporic relative of Physoderma (Blastocladiomycota). *Mycotaxon*, 118, pp.177–180.

Jobard, M., Rasconi, S. & Sime-Ngando, T., 2010. Fluorescence in situ hybridization of uncultured zoosporic fungi: Testing with clone-FISH and application to freshwater samples using CARD-FISH. *Journal of Microbiological Methods*, 83(2), pp.236–243. Available at: http://dx.doi.org/10.1016/j.mimet.2010.09.006.

John, H.A., Birnstiel, M.L. & Jones, K.W., 1969. RNA-DNA hybrids at the cytological level. *Nature*, 223(5206), pp.582–7. Available at: http://www.ncbi.nlm.nih.gov/pubmed/5799530.

Kagami, M. et al., 2004. Daphnia can protect diatoms from fungal parasitism. *Limnology and Oceanography*, 49(3), pp.680–685. Available at: http://doi.wiley.com/10.4319/lo.2004.49.3.0680.

Kakizono, T., Kobayashi, M. & Nagai, S., 1992. Effect of carbon/nitrogen ratio on encystment accompanied with astaxanthin formation in a green alga, Haematococcus pluvialis. *Journal of Fermentation and Bioengineering*, 74(6), pp.403–405.

Kemp, P.F., Lee, S. & Laroche, J., 1993. Estimating the growth rate of slowly growing marine bacteria from RNA content. *Applied and environmental microbiology*, 59(8), pp.2594–601. Available at: http://www.ncbi.nlm.nih.gov/pubmed/16349018.

Kline, R.B., 2011. *Principles and Practice of Structural Equation Modeling* 3rd ed. The Guilford Press, ed., New York. Available at: http://www.imd.inder.cu/adjuntos/article/521/Principles and Practice of Structural Equation Modeling.pdf.

Koller, M., Muhr, A. & Braunegg, G., 2014. Microalgae as versatile cellular factories for valued products. *Algal Research*, 6, pp.52–63.

Koshkin, A.A. et al., 1998. LNA (Locked Nucleic Acid): An RNA Mimic Forming Exceedingly Stable LNA:LNA Duplexes.

Koyabashi, M. et al., 1992. Effects of Light Intensity, light quality and illumination cycle on astaxantin formation in a green alga, Haematococcus pluvialis. *Journal of Fermentation and Bioengineering*, 74(1), pp.61–63.

Kudoh, S. & Tokahashi, M., 1990. Fungal control of population changes of the planktonic diatom asterionella formosa in a shallow eutrophic lake. *Journal of Phycology*, 26(2), pp.239–244. Available at: http://doi.wiley.com/10.1111/j.0022-3646.1990.00239.x.

Lehninger, 1871. Biochemistry.

Lemoine, Y. & Schoefs, B., 2010. Secondary ketocarotenoid astaxanthin biosynthesis in algae: a multifunctional response to stress. *Photosynthesis Research*, 106(1–2), pp.155–177. Available at: http://link.springer.com/10.1007/s11120-010-9583-3.

Letcher, P.M. et al., 2013. Characterization of Amoeboaphelidium protococcarum, an algal parasite new to the cryptomycota isolated from an outdoor algal pond used for the production of biofuel. *PloS one*, 8(2), p.e56232. Available at: http://www.ncbi.nlm.nih.gov/pubmed/23437098.

Levsky, J.M. & Singer, R.H., 2003. Fluorescence in situ hybridization: past, present and future. *Journal of Cell Science*, 116(14), pp.2833–2838. Available at: http://jcs.biologists.org/cgi/doi/10.1242/jcs.00633.

Li, Y. et al., 2008. Consumption of oxygen by astaxanthin biosynthesis: A protective mechanism against oxidative stress in Haematococcus pluvialis (Chlorophyceae). *Journal of Plant Physiology*, 165(17), pp.1783–1797. Available at: http://www.ncbi.nlm.nih.gov/pubmed/18313796.

Li, Y. et al., 2010. Effect of photon flux densities on regulation of carotenogenesis and cell viability of Haematococcus pluvialis (Chlorophyceae). *Journal of Applied Phycology*, 22(3), pp.253–263.

Lipoglavsek, L. & Avgustin, G., 2001. Application of Flow Cytometry for Ecological Monitoring of the Rumen Microbial Ecosystem - Journals - NCBI. *Folia Microbiol (Praha)*, 46(1), pp.53–55. Available at: https://www.ncbi.nlm.nih.gov/labs/articles/11501477/.

Loike, J.D. & Silverstein, S.C., 1983. A fluorescence quenching technique using trypan blue to differentiate between attached and ingested glutaraldehyde-fixed red blood cells in phagocytosing murine macrophages. *Journal of immunological methods*, 57(1–3), pp.373–9. Available at: http://www.ncbi.nlm.nih.gov/pubmed/6402550.

Lorenz, R.T. et al., 2000. Commercial potential for Haematococcus microalgae as a natural source of astaxanthin. *Trends in biotechnology*, 18(4), pp.160–7. Available at: http://www.ncbi.nlm.nih.gov/pubmed/10740262.

Lunet, N., Severo, M. & Barros, H., 2008. Inferência estatística: intervalos de confiança vs. testes de hipóteses. *Revista Portuguesa de Cirurgia*, 2(5), pp.33–40. Available at: https://mail.google.com/mail/u/0/#inbox/15c89abb808d2204?projector=1.

Ma, R.Y.-N. & Chen, F., 2001. Enhanced production of free trans-astaxanthin by oxidative stress in the cultures of the green microalga Chlorococcum sp. *Process Biochemistry*, 36(12), pp.1175–1179. Available at: http://www.sciencedirect.com/science/article/pii/S0032959201001571.

Margalith, P.Z., 1999. Production of ketocarotenoids by microalgae. *Applied Microbiology and Biotechnology*, 51(4), pp.431–438. Available at: http://link.springer.com/10.1007/s002530051413.

Margo, C.E. et al., 1967. The diagnostic value of fungal autofluorescence. *Survey of ophthalmology*, 29(5), pp.374–6. Available at: http://www.ncbi.nlm.nih.gov/pubmed/3992475.

Markou, G. & Nerantzis, E., 2013. Microalgae for high-value compounds and biofuels production: A review with focus on cultivation under stress conditions. *Biotechnology Advances*, 31(8), pp.1532–1542.

Mateo-Mart, E. & Pradier, C.-M., 2010. A Novel Type of Nucleic Acid-based Biosensors: the Use of PNA Probes, Associated with Surface Science and Electrochemical Detection Techniques. In *Intelligent and Biosensors*. InTech. Available at: http://www.intechopen.com/books/intelligent-and-biosensors/a-novel-type-of-nucleic-acid-based-biosensors-the-use-of-pna-probes-associated-with-surface-science-.

McBride, R. et al., 2013. Use of fungicides in liquid systems.

Mostafa, S.S.M., 2012. Microalgal Biotechnology: Prospects and Applications. In *Plant Science*. Giza, pp. 275–314. Available at: http://dx.doi.org/10.5772/53649.

Moter, A. & Göbel, U.B., 2000. Fluorescence in situ hybridization (FISH) for direct visualization of microorganisms. *Journal of Microbiological Methods*, 41(2), pp.85–112.

Mulbry, W. et al., 2004. Recycling of manure nutrients: use of algal biomass from dairy manure treatment as a slow release fertilizer. *Bioresource Technology*, 96, pp.451–458.

Mulbry, W. et al., 2008. Treatment of dairy manure effluent using freshwater algae: Algal productivity and recovery of manure nutrients using pilot-scale algal turf scrubbers. *Bioresource Technology*, 99, pp.8137–8142.

Naguib, Y.M.A., 2000. Antioxidant Activities of Astaxanthin and Related Carotenoids. *Journal of Agricultural and Food Chemistry*, 48(4), pp.1150–1154. Available at: http://pubs.acs.org/doi/abs/10.1021/jf991106k.

Neumann, M. & Gabel, D., 2002. Simple Method for Reduction of Autofluorescence in Fluorescence Microscopy. *The Journal of Histochemistry & Cytochemistry*, 50(3), pp.437–439. Available at: http://www.jhc.org.

Nielsen, P. et al., 1991. Sequence-selective recognition of DNA by strand displacement with a thymine-substituted polyamide. *Science*, 254(5037).

Nielsen, P.E., 2001. Peptide nucleic acid: a versatile tool in genetic diagnostics and molecular biology. *Current opinion in biotechnology*, 12(1), pp.16–20. Available at: http://www.ncbi.nlm.nih.gov/pubmed/11167067.

Nielsen, P.E. & Egholm, M., 1999. An Introduction to Peptide Nucleic Acid. *Current Issues Molec. Biol.*, 1(2), pp.89–104.

Oliveira, V.C. et al., 2010. Sudan Black B treatment reduces autofluorescence and improves resolution of in situ hybridization specific fluorescenct signals of brain sections. *Histology and Histopathology*, 25, pp.1017–1024.

Panis, G. & Rosales Carreon, J., 2016. Commercial astaxanthin production derived by green alga Haematococcus pluvialis: A microalgae process model and a techno-economic assessment all trough production line. *Algal Research*, 18, pp.175–190.

Pardue, M.L. & Gall, J.G., 1969. Molecular hybridization of radioactive DNA to the DNA of cytological preparations. *Proceedings of the National Academy of Sciences of the United States of America*, 64(2), pp.600–4.

Pérez-López, P. et al., 2014. Life cycle assessment of the production of the red antioxidant carotenoid astaxanthin by microalgae: from lab to pilot scale. *Journal of Cleaner Production*, 64, pp.332–344.

Pernthaler, A., Pernthaler, J. & Amann, R., 2002. Fluorescence In Situ Hybridization and Catalyzed Reporter Deposition for the Identification of Marine Bacteria. *Applied and Environmental Microbiology*, 68(6), pp.3094–3101. Available at: https://www.ncbi.nlm.nih.gov/pmc/articles/PMC123953/pdf/1927.pdf.

Perry-O'Keefe, H. et al., 2001. Identification of indicator microorganisms using a standardized PNA FISH method. *Journal of microbiological methods*, 47(3), pp.281–92. Available at: http://www.ncbi.nlm.nih.gov/pubmed/11714518.

Petersen, M. et al., 2003. LNA: a versatile tool for therapeutics and genomics. *Trends in biotechnology*, 21(2), pp.74–81. Available at: http://www.ncbi.nlm.nih.gov/pubmed/12573856.

Pinkel, D. et al., 1988. Fluorescence in situ hybridization with human chromosome-specific libraries: detection of trisomy 21 and translocations of chromosome 4. *Proceedings of the National Academy of Sciences of the United States of America*, 85(23), pp.9138–9142. Available at: http://www.ncbi.nlm.nih.gov/pubmed/2973607.

Pinkel, D., Straume, T. & Gray, J.W., 1986. Cytogenetic analysis using quantitative, high-sensitivity, fluorescence hybridization. *Proceedings of the National Academy of Sciences of the United States of America*, 83(9), pp.2934–2938. Available at: http://www.ncbi.nlm.nih.gov/pubmed/3458254.

Porter, T.M. et al., 2011. Molecular phylogeny of the Blastocladiomycota (Fungi) based on nuclear ribosomal DNA. *Fungal Biology*, 115(4–5), pp.381–392. Available at: http://www.ncbi.nlm.nih.gov/pubmed/21530920.

Poulsen, L.K., Ballard, G. & Stahl, D.A., 1993. Use of rRNA fluorescence in situ hybridization for measuring the activity of single cells in young and established biofilms. *Applied and environmental microbiology*, 59(5), pp.1354–60. Available at: http://www.ncbi.nlm.nih.gov/pubmed/7685999.

Qin, S., Liu, G.-X. & Hu, Z.-Y., 2008. The accumulation and metabolism of astaxanthin in Scenedesmus obliquus (Chlorophyceae). *Process Biochemistry*, 43(8), pp.795–802. Available at: http://www.sciencedirect.com/science/article/pii/S1359511308001074.

Rasconi, S. et al., 2009. Use of calcofluor white for detection, identification, and quantification of phytoplanktonic fungal parasites. *Applied and environmental microbiology*, 75(8), pp.2545–2553. Available at: http://www.ncbi.nlm.nih.gov/pubmed/19233954.

Richmond, A., 2004. *Handbook of microalgal culture : biotechnology and applied phycology*, Blackwell Science.

Rothman, J., 1978. A Show of Confidence. *New England Journal of Medicine*, 299(24), pp.1362–1363. Available at: http://www.ncbi.nlm.nih.gov/pubmed/362205 [Accessed June 9, 2017].

Rudkin, G.T. & Stollar, B.D., 1977. High resolution detection of DNA–RNA hybrids in situ by indirect immunofluorescence. *Nature*, 265(5593), pp.472–473. Available at: http://www.nature.com/doifinder/10.1038/265472a0.

Sarada, R., Tripathi, U. & Ravishankar, G., 2002. Influence of stress on astaxanthin production in Haematococcus pluvialis grown under different culture conditions. *Process Biochemistry*, 37, pp.623–627. Available at: http://www.sciencedirect.com/science/article/pii/S0032959201002461.

Schnell, S.A., Staines, W.A. & Wessendorf, M.W., 1999. Reduction of Lipofuscin-like Autofluorescence in Fluorescently Labeled Tissue. *The Journal of Histochemistry & Cytochemistry*, 47(6), pp.719–730. Available at: http://www.jhc.org.

Schönhuber, W. et al., 1999. In Situ Identification of Cyanobacteria with Horseradish Peroxidase-Labeled, rRNA-Targeted Oligonucleotide Probes. *APPLIED AND ENVIRONMENTAL MICROBIOLOGY*, 65(3), pp.1259–1267.

Sen, A. & Nielsen, P.E., 2006. Unique Properties of Purine/Pyrimidine Asymmetric PNA:DNA Duplexes: Differential Stabilization of PNA:DNA Duplexes by Purines in the PNA Strand. *Biophysical Journal*, 90, pp.1329–1337. Available at: https://www.ncbi.nlm.nih.gov/pmc/articles/PMC1367284/pdf/1329.pdf.

Shah, M.M.R. et al., 2016. Astaxanthin-Producing Green Microalga Haematococcus pluvialis: From Single Cell to High Value Commercial Products. *Frontiers in Plant Science*, 7(531), pp.1–28.

Shakeel, S., Karim, S. & Ali, A., 2006. Peptide nucleic acid (PNA) - A review. *Journal of Chemical Technology and Biotechnology*, 81(6), pp.892–899.

Shapiro, S.S. & Wilk, M.B., 1965. An analysis of variance test for normality (complete samples). *Biometrika*, 52(3–4), pp.591–611. Available at: https://academic.oup.com/biomet/article-lookup/doi/10.1093/biomet/52.3-4.591.

Shin, W., Boo, S.M. & Longcore, J.E., 2001. Entophlyctis apiculata, a chytrid parasite of Chlamydomonas sp. (Chlorophyceae). *Canadian Journal of Botany*, 79(9), pp.1083–1089. Available at: http://www.nrcresearchpress.com/doi/abs/10.1139/b01-086.

Shurin, J.B. et al., 2013. Industrial-strength ecology: trade-offs and opportunities in algal biofuel production J. Grover, ed. *Ecology Letters*, 16(11), pp.1393–1404. Available at: http://doi.wiley.com/10.1111/ele.12176.

Sieracki, C.K., Sieracki, M.E. & Yentsch, C.S., 1998. An imaging-in-flow system for automated analysis of marine microplankton. *Marine Ecology Progress Series*, 168, pp.285–296.

Silverman, A.P. & Kool, E.T., 2007. Oligonucleotide Probes for RNA-Targeted Fluorescence In Situ Hybridization. *Advances in Clinical Chemistry*, 43(November), pp.79–115.

Song, L. et al., 1995. Photobleaching kinetics of fluorescein in quantitative fluorescence microscopy. *Biophysical Journal*, 68, pp.2588–2600. Available at: http://www.cell.com/biophysj/pdf/S0006-3495(95)80442-X.pdf.

Stender, H. et al., 2002. PNA for rapid microbiology. *Journal of Microbiological Methods*, 48(1), pp.1–17.

Strittmatter, M. et al., 2016. A new flagellated dispersion stage in Paraphysoderma sedebokerense, a pathogen of Haematococcus pluvialis. *Journal of Applied Phycology*, 28(3), pp.1553–1558. Available at: http://dx.doi.org/10.1007/s10811-015-0700-8.

Tjahjono, A. et al., 1994. Hyper-accumulation of astaxanthin in a green alga Haematococcus pluvialis at elevated temperatures.

Tsien, R.Y., Ernst, L. & Waggoner, A., 2006. Fluorophores for Confocal Microscopy: Photophysics and Photochemistry. In James B. Pawley, ed. *The Handbook for Biological Confocal Microscopy*. New York: Springer Science+Business Media, p. 338-. Available at: http://wwwuser.gwdg.de/~uboehm/images/16.pdf.

Wagner, M. et al., 1998. In situ detection of a virulence factor mRNA and 16S rRNA in Listeria monocytogenes. *FEMS Microbiol Lett*, 160, pp.159–168.

Wagner, M., Horn, M. & Daims, H., 2003. Fluorescence in situ hybridisation for the identification and characterisation of prokaryotes. *Current Opinion in Microbiology*, 6(3), pp.302–309.

Wallner, G., Amann, R. & Beisker, W., 1993. Optimizing fluorescent in situ hybridization with rRNA-targeted oligonucleotide probes for flow cytometric identification of microorganisms. *Cytometry*, 14(2), pp.136–143. Available at: http://doi.wiley.com/10.1002/cyto.990140205.

Wang, H. et al., 2013. The contamination and control of biological pollutants in mass cultivation of microalgae. *Bioresource Technology*, 128, pp.745–750. Available at: http://dx.doi.org/10.1016/j.biortech.2012.10.158.

Wilkinson, I.J. et al., 1990. Problems Associated with Identification of Legionella Species from the Environment and Isolation of Six Possible New Species. *Applied and Environmental Microbiology*, 56(3), pp.796–802.

Yazbeck, D.R., Min, K.-L. & Damha, M.J., 2002. Molecular requirements for degradation of a modified sense RNA strand by Escherichia coli ribonuclease H1. *Nucleic acids research*, 30(14), pp.3015–3025. Available at: http://www.pubmedcentral.nih.gov/articlerender.fcgi?artid=135749&tool=pmcentrez&rendertype=abstract.

Yilmaz, L.S. & Noguera, D.R., 2004. Mechanistic Approach to the Problem of Hybridization Efficiency in Fluorescent In Situ Hybridization. *Applied and Environmental Microbiology*, 70(12), pp.7126–7139. Available at: https://www.ncbi.nlm.nih.gov/pmc/articles/PMC535158/pdf/0654-04.pdf.

Yilmaz, L.S., Ökten, H.E. & Noguera, D.R., 2006. Making All Parts of the 16S rRNA of Escherichia coli Accessible In Situ to Single DNA Oligonucleotides Making All Parts of the 16S rRNA of Escherichia coli Accessible In Situ to Single DNA Oligonucleotides †. *Applied and Environmental Microbiology*, 72(1), pp.733–744.

Zhang, J. et al., 2013. Production method and device for preventing and treating contamination of paraphysoderma sedebokerensis in haematococcus pluvialis.

Zhang, W. et al., 2014. Attached cultivation of Haematococcus pluvialis for astaxanthin production.

Zhang, X. et al., 2007. Impact of astaxanthin-enriched algal powder of Haematococcus pluvialis on memory improvement in BALB/c mice. *Environmental Geochemistry and Health*, 29(6), pp.483–489. Available at: http://link.springer.com/10.1007/s10653-007-9117-x.

Appendix A1. Culture media composition

Table A1 1. Bold Basal Medium with 3-fold Nitrogen and Vitamins (3N-BBM+V) *Haematococcus pluvialis* growth medium composition. The Chytrid Growth Medium for *Paraphysoderma sedebokerense* is 3N-BBM+V supplemented with 0.25 g/L of yeast extract, 0.25 g/L of peptone and 5 g/L of glucose. For solid medium use 1.5% (wt/vol) agar

Stocks	Bold Basal Medium with 3-fold Nitrogen and Vitamins
$NaNO_3$ (75.0 g/l)	10 mL/L
$CaCl_2.2H_2O$ (2.5 g/l)	10 mL/L
$MgSO_4.7H_2O$ (7.5 g/l)	10 mL/L
$K_2HPO_4.3\ H_2O$ (7.5 g/l)	10 mL/L
KH_2PO_4 (17.5 g/l)	10 mL/L
NaCl (2.5 g/l)	10 mL/L
Trace elements:	
Na_2EDTA (0.25 g/l)	
$FeCl_3.6H_2O$ (97.0 mg)	
$MnCl_2.4H_2O$ (41.0 mg)	6 mL/L
$ZnCl_2$ (5.0 mg)	
$CoCl_2.6H_2O$ (2.0 mg)	
$Na_2MoO_4.2H_2O$ (4.0 mg)	
Vitamin B_1 (1.2 g/l)	1 mL/L
Vitamin B_{12} (1 g/l)	1 mL/L

Appendix A2. Designed probe characteristics

Table A2 1. Complementary sequences to the designed PNA-probe

rRNA		
Blast description	**Organism**	**Type**
Paraphysoderma sedebokerense isolate PS1 18S ribosomal RNA gene, partial sequence	*Paraphysoderma sedebokerense*	Fungus
Paraphysoderma sedebokerense isolate FD61 18S ribosomal RNA gene, partial sequence	*Paraphysoderma sedebokerense*	Fungus
Blastocladiales sp. TJ-2007a 18S ribosomal RNA gene, partial sequence	*Blastocladiales sp.*	Fungus
Chlamydomonas debaryana strain mn0727 18S ribosomal RNA gene, partial sequence	*Chlamydomonas debaryana*	Algae
mRNA		
Blast description	**Organism**	**Type**
Aphanomyces invadans hypothetical protein partial mRNA	*Aphanomyces invadans*	Fungus
Aspergillus nomius NRRL 13137 NRPS-like enzyme mRNA	*Aspergillus nomius*	Fungus
Bipolaris maydis ATCC 48331 carbohydrate esterase family 16 protein partial mRNA	*Bipolaris maydis*	Fungus
Bipolaris oryzae ATCC 44560 carbohydrate esterase family 16 protein partial mRNA	*Bipolaris oryzae*	Fungus
Capronia epimyces CBS 606.96 hypothetical protein partial mRNA	*Capronia epimyces*	Fungus
Chondrus crispus unnamed protein product (CHC_T00001877001) mRNA, complete cds	*Chondrus crispus*	Algae
Cochliobolus sativus ND90Pr carbohydrate esterase family 16 protein partial mRNA	*Cochliobolus sativus*	Fungus
Fusarium oxysporum f. sp. lycopersici 4287 hypothetical protein mRNA	*Fusarium oxysporum*	Fungus
Gaeumannomyces graminis var. tritici R3-111a-1 kinase isozyme 4 mRNA	*Gaeumannomyces graminis*	Fungus
Moniliophthora roreri MCA 2997 1,3-beta-glucansynthase partial mRNA	*Moniliophthora roreri*	Fungus
Myceliophthora thermophila ATCC 42464 hypothetical protein (MYCTH_2312042) mRNA, complete cds	*Myceliophthora thermophila*	Fungus
Nectria haematococca mpVI 77-13-4 predicted protein, mRNA	*Nectria haematococca*	Fungus
Podospora anserina S mat+ hypothetical protein (PODANSg4764) partial mRNA	*Podospora anserina*	Fungus
Podospora anserina S mat+ hypothetical protein (PODANSg8235) partial mRNA	*Podospora anserina*	Fungus
Sphaerulina musiva SO2202 FAD/NAD(P)-binding domain-containing protein mRNA	*Sphaerulina musiva*	Fungus
Tilletiaria anomala UBC 951 hypothetical protein mRNA	*Tilletiaria anomala*	Fungus
Verruconis gallopava hypothetical protein mRNA	*Verruconis gallopava*	Fungus

Verruconis gallopava hypothetical protein, variant 1 mRNA	*Verruconis gallopava*	Fungus
Verruconis gallopava hypothetical protein, variant 2 mRNA	*Verruconis gallopava*	Fungus

Cromossome/genome		
Blast description	**Organism**	**Type**
Acinetobacter guillouiae DNA, complete geonome, strain: NBRC 110550	*Acinetobacter guillouiae*	
Acinetobacter johnsonii XBB1, complete genome	*Acinetobacter johnsonii*	
Anaerolinea thermophila UNI-1 DNA, complete genome	*Anaerolinea thermophila*	
Anaplasma phagocytophilum HZ, complete genome	*Anaplasma phagocytophilum*	
Anaplasma phagocytophilum str. Dog2 genome	*Anaplasma phagocytophilum*	
Anaplasma phagocytophilum str. HZ2, complete genome	*Anaplasma phagocytophilum*	
Anaplasma phagocytophilum str. JM, complete genome	*Anaplasma phagocytophilum*	
Burkholderia sp. CCGE1002 chromosome 2, complete sequence	*Burholderia sp*	
Caldivirga maquilingensis IC-167, complete genome	*Caldivirga maquilingensis*	
Comamonadaceae bacterium A1 DNA, complete genome	*Comamonadaceae bacteium*	
Comamonas testosteroni P19 genome assembly Comamonas testosteroni P19, chromosome : I	*Comamonas testosteroni*	
Fusobacterium nucleatum subsp. animalis 7_1, complete genome	*Fusbacterium nucleatum*	
Fusobacterium nucleatum subsp. vincentii ChDC F8 strain KCOM 1231, complete genome	*Fusbacterium nucleatum*	
Lactobacillus paracasei N1115, complete genome	*Lactobacillus paracasei*	
Lactobacillus paracasei strain CAUH35, complete genome	*Lactobacillus paracasei*	
Lactobacillus paracasei subsp. paracasei JCM 8130 DNA, complete genome	*Lactobacillus paracasei*	
Leptosphaeria maculans brassicae wa74_scaffold00238 complete sequence	*Leposphaeria maculans*	
Leptosphaeria maculans brassicae wa74_scaffold00734 complete sequence	*Leposphaeria maculans*	
Leptosphaeria maculans JN3 SuperContig_17_v2	*Leposphaeria maculans*	
Mannheimia sp. USDA-ARS-USMARC-1261, complete genome	*Mannheimia sp*	
Myceliophthora thermophila ATCC 42464 chromosome 7, complete sequence	*Mycliophthora thermophila*	
Pelobacter propionicus DSM 2379 plasmid pPRO1, complete sequence	*Pelbacter propionicus*	
Podospora anserina genomic DNA, chromosome 2	*Podospora anserina*	
Podospora anserina genomic DNA, chromosome 7	*Podospora anserina*	

Podospora anserina S mat+ genomic DNA chromosome 2, supercontig 2	*Podospora anserina*
Podospora anserina S mat+ genomic DNA chromosome 7, supercontig 1	*Podospora anserina*
Propionibacterium propionicum F0230a, complete genome	*Propionibacterium propionicum*
Pseudoalteromonas luteoviolacea strain S4054 chromosome 2, complete sequence	*Psedoalteromonas luteoviolacea*
Pseudoalteromonas luteoviolacea strain S40542 chromosome 2, complete sequence	*Psedoalteromonas luteoviolacea*
Pseudoalteromonas luteoviolacea strain S4054249 chromosome 2, complete sequence	*Psedoalteromonas luteoviolacea*
Shewanella woodyi ATCC 51908, complete genome	*Shewanella woodyi*
Sideroxydans lithotrophicus ES-1, complete genome	*Sideroxydans lithotrophicus*
Streptococcus oralis Uo5 complete genome sequence	*Streptococcus orails*
Thioflavicoccus mobilis 8321, complete genome	*Thioflavicoccus mobilis*
TPA: Aspergillus nidulans FGSC A4 chromosome VII	*Aspergillus nidulans*
Uncultured Candidatus Thalassoarchaea euryarchaeote clone MedDCM-OCT2007-C866 genomic sequence	*Thalassoarchae*
Verticillium dahliae JR2 chromosome 1, complete sequence	*Vericillium dahliae*
Verticillium dahliae VdLs.17 chromosome 2, complete sequence	*Vericillium dahliae*
Waddlia chondrophila 2032/99 annotated genome fragment, clone 1103163150312	*Wadlia chondrophila*
Waddlia chondrophila WSU 86-1044, complete genome	*Wadlia chondrophila*

Appendix A3. Student's *t* Test for probe specificity testing

Table A3 1. Shapiro-Wilk' test of normality for the samples of *Saccharomyces cerevisae*, treated with the probe and without the probe. To assume normality the significance (sig) needs to be superior to 0.050, df represent the degrees of freedom

Tests of Normality

	Kolmogorov-Smirnov[a]			Shapiro-Wilk		
	Statistic	df	Sig.	Statistic	df	Sig.
S.cerevisae_probe	,214	6	,200*	,925	6	,539
S.cerevisae_control	,238	6	,200*	,917	6	,484

*. This is a lower bound of the true significance.

a. Lilliefors Significance Correction

Table A3 2. Shapiro-Wilk' test of normality for the samples of *Haematococcus pluvialis*, treated with the probe and without the probe. To assume normality the significance (sig) needs to be superior to 0.050, df represent the degrees of freedom

Tests of Normality

	Kolmogorov-Smirnov[a]			Shapiro-Wilk		
	Statistic	df	Sig.	Statistic	df	Sig.
H.pluvialis_probe	,395	14	,000	,653	14	,000
H.pluvialis_control	,328	14	,000	,749	14	,001

a. Lilliefors Significance Correction

Table A3 3. Statistics description for samples of *Haematococcus pluvialis* treated with and without the probe. To assume normality the Skewness needs to be below 3 and the Kurtosis below 7

Descriptives

			Statistic	Std. Error
H.pluvialis_probe	Mean		84,7625	,17929
	95% Confidence Interval for Mean	Lower Bound	84,3752	
		Upper Bound	85,1498	
	5% Trimmed Mean		84,8070	
	Median		84,9720	
	Variance		,450	
	Std. Deviation		,67083	
	Minimum		83,17	
	Maximum		85,55	
	Range		2,38	
	Interquartile Range		,16	
	Skewness		-1,949	,597
	Kurtosis		3,095	1,154
H.pluvialis_control	Mean		84,8756	,07947
		Lower Bound	84,7040	

95% Confidence Interval for Mean	Upper Bound	85,0473
5% Trimmed Mean		84,8879
Median		84,9995
Variance		,088
Std. Deviation		,29733
Minimum		84,24
Maximum		85,29
Range		1,05
Interquartile Range		,15
Skewness		-1,473 ,597
Kurtosis		1,732 1,154

Table A3 4. Statistics information for the intensity of fluorescence of *Saccharomyces cerevisae* treated with and without the probe

Paired Samples Statistics

		Mean	N	Std. Deviation	Std. Error Mean
Pair 1	S.cerevisae_probe	21,2438	6	2,71811	1,10966
	S.cerevisae_control	22,5120	6	3,69672	1,50918

Table A3 5. Statistics information for the intensity of fluorescence of *Haematococcus pluvialis* treated with and without the probe

Paired Samples Statistics

		Mean	N	Std. Deviation	Std. Error Mean
Pair 1	H.pluvialis_probe	84,7625	14	,67083	,17929
	H.pluvialis_control	84,8756	14	,29733	,07947

Table A3 6. Student's *t* Test between the samples with and without the probe for *Saccharomyces cerevisae*. For significant differences between the probe and the control the significance (sig.) needs to be equal or below 0.05, df represent the degrees of freedom

Paired Samples Test

		Paired Differences					t	df	Sig. (2-tailed)
		Mean	Std. Deviation	Std. Error Mean	95% Confidence Interval of the Difference Lower	Upper			
Pair 1	S.cerevisae_probe - S.cerevisae_control	-1,26817	4,87854	1,99165	-6,38788	3,85154	-,637	5	,552

Table A3 7. Student's *t* Test between the samples with and without the probe for *Haematococcus pluvialis*. For significant differences between the probe and the control the significance needs to be equal or below 0.05, df represent the degrees of freedom

Paired Samples Test

		Paired Differences					t	df	Sig. (2-tailed)
		Mean	Std. Deviation	Std. Error Mean	95% Confidence Interval of the Difference				
					Lower	Upper			
Pair 1	H.pluvialis_probe - H.pluvialis_control	-,11314	,68847	,18400	-,51065	,28437	-,615	13	,549

Appendix A4. Statistics for protocol optimization

Table A4 1. Shapiro-Wilk' test of normality for the samples at different temperatures from 50 to 60 ºC, treated with the probe. To assume normality the significance (sig) needs to be superior to 0.050, df represent the degrees of freedom

Tests of Normality

	Kolmogorov-Smirnov[a]			Shapiro-Wilk		
	Statistic	df	Sig.	Statistic	df	Sig.
Temperature50_probe	,315	52	,000	,625	52	,000
Temperature52_probe	,239	52	,000	,841	52	,000
Temperature54_probe	,248	52	,000	,838	52	,000
Temperature56_probe	,168	52	,001	,908	52	,001
Temperature58_probe	,234	52	,000	,835	52	,000
Temperature60_probe	,267	52	,000	,800	52	,000

a. Lilliefors Significance Correction

Table A4 2. Statistics description for samples at different temperatures treated with the probe. To assume normality the Skewness needs to be below 3 and the Kurtosis below 7

Descriptives

			Statistic	Std. Error
Temperature50_probe	Mean		17,4862	2,95259
	95% Confidence Interval for Mean	Lower Bound	11,5586	
		Upper Bound	23,4137	
	5% Trimmed Mean		14,6111	
	Median		8,7450	
	Variance		453,326	
	Std. Deviation		21,29145	
	Minimum		1,19	
	Maximum		90,26	
	Range		89,07	
	Interquartile Range		12,95	
	Skewness		2,352	,330
	Kurtosis		4,798	,650
Temperature52_probe	Mean		32,2144	3,87341
	95% Confidence Interval for Mean	Lower Bound	24,4382	
		Upper Bound	39,9906	
	5% Trimmed Mean		30,4638	
	Median		23,4400	
	Variance		780,173	
	Std. Deviation		27,93157	

	Minimum	5,67	
	Maximum	93,10	
	Range	87,43	
	Interquartile Range	46,10	
	Skewness	,658	,330
	Kurtosis	-,887	,650
Temperature54_probe	Mean	36,7075	4,08407
	95% Confidence Interval for Mean Lower Bound	28,5084	
	95% Confidence Interval for Mean Upper Bound	44,9066	
	5% Trimmed Mean	35,0277	
	Median	20,4550	
	Variance	867,339	
	Std. Deviation	29,45062	
	Minimum	7,67	
	Maximum	100,07	
	Range	92,40	
	Interquartile Range	53,23	
	Skewness	,609	,330
	Kurtosis	-1,110	,650
Temperature56_probe	Mean	37,0129	3,02291
	95% Confidence Interval for Mean Lower Bound	30,9441	
	95% Confidence Interval for Mean Upper Bound	43,0816	
	5% Trimmed Mean	36,4418	
	Median	39,6850	
	Variance	475,174	
	Std. Deviation	21,79849	
	Minimum	6,57	
	Maximum	77,00	
	Range	70,43	
	Interquartile Range	38,72	
	Skewness	,201	,330
	Kurtosis	-1,319	,650
Temperature58_probe	Mean	29,9548	3,32799
	95% Confidence Interval for Mean Lower Bound	23,2736	
	95% Confidence Interval for Mean Upper Bound	36,6360	
	5% Trimmed Mean	28,5485	
	Median	17,5100	
	Variance	575,926	
	Std. Deviation	23,99845	
	Minimum	6,88	
	Maximum	83,98	
	Range	77,10	

	Interquartile Range	43,40	
	Skewness	,713	,330
	Kurtosis	-,992	,650
Temperature60_probe	Mean	21,8485	2,48976
	95% Confidence Interval for Mean Lower Bound	16,8501	
	95% Confidence Interval for Mean Upper Bound	26,8469	
	5% Trimmed Mean	20,7313	
	Median	9,5100	
	Variance	322,343	
	Std. Deviation	17,95393	
	Minimum	5,98	
	Maximum	59,66	
	Range	53,68	
	Interquartile Range	30,24	
	Skewness	,776	,330
	Kurtosis	-,967	,650

Table A4 3. Mauchly's Test of Sphericity for the samples treated with the probe. To assume sphericity the significance (sig) needs to be superior to 0.050, df represent the degrees of freedom

Mauchly's Test of Sphericity[a]

Measure: MEASURE_1

Within Subjects Effect	Mauchly's W	Approx. Chi-Square	df	Sig.	Epsilon[b]		
					Greenhouse-Geisser	Huynh-Feldt	Lower-bound
Temperature	,445	39,767	14	,000	,791	,866	,200

Tests the null hypothesis that the error covariance matrix of the orthonormalized transformed dependent variables is proportional to an identity matrix.

a. Design: Intercept

Within Subjects Design: Temperature

b. May be used to adjust the degrees of freedom for the averaged tests of significance. Corrected tests are displayed in the Tests of Within-Subjects Effects table.

Table A4 4. Tests of Sphericity for the samples treated with the probe. For data populations below 30 the Greenhouse-Geisser approximation may be used. The significance (sig.) should be below 0.05 and df represent the degrees of freedom

Tests of Within-Subjects Effects

Measure: MEASURE_1

Source		Type III Sum of Squares	df	Mean Square	F	Sig.
Temperature	Sphericity Assumed	16552,610	5	3310,522	14,390	,000
	Greenhouse-Geisser	16552,610	3,955	4185,686	14,390	,000
	Huynh-Feldt	16552,610	4,329	3824,064	14,390	,000
	Lower-bound	16552,610	1,000	16552,610	14,390	,000
Error(Temperature)	Sphericity Assumed	58664,352	255	230,056		
	Greenhouse-Geisser	58664,352	201,683	290,874		
	Huynh-Feldt	58664,352	220,755	265,744		
	Lower-bound	58664,352	51,000	1150,281		

Table A4 5. Statistics information for the different temperatures treated with the probe. Temperature 1, 2, 3, 4, 5, and 6 corresponds, respectively to 50, 52, 54, 56, 58 and 60

Estimates

Measure: MEASURE_1

Temperature	Mean	Std. Error	95% Confidence Interval	
			Lower Bound	Upper Bound
1	17,486	2,953	11,559	23,414
2	32,214	3,873	24,438	39,991
3	36,707	4,084	28,508	44,907
4	37,013	3,023	30,944	43,082
5	29,955	3,328	23,274	36,636
6	21,848	2,490	16,850	26,847

Table A4 6. ANOVA test between the different temperatures. Temperature 1, 2, 3, 4, 5, and 6 corresponds, respectively to 50, 52, 54, 56, 58 and 60

Pairwise Comparisons

Measure: MEASURE_1

(I) Temperature	(J) Temperature	Mean Difference (I-J)	Std. Error	Sig.[b]	95% Confidence Interval for Difference[b]	
					Lower Bound	Upper Bound
1	2	-14,728*	3,072	,000	-20,895	-8,561
	3	-19,221*	3,961	,000	-27,173	-11,270
	4	-19,527*	2,665	,000	-24,876	-14,177
	5	-12,469*	2,978	,000	-18,447	-6,490
	6	-4,362	3,525	,222	-11,439	2,715

2	1	14,728*	3,072	,000	8,561	20,895
	3	-4,493	3,039	,145	-10,595	1,608
	4	-4,798*	2,203	,034	-9,222	-,375
	5	2,260	2,578	,385	-2,915	7,435
	6	10,366*	2,956	,001	4,432	16,300
3	1	19,221*	3,961	,000	11,270	27,173
	2	4,493	3,039	,145	-1,608	10,595
	4	-,305	2,928	,917	-6,183	5,572
	5	6,753*	3,217	,041	,295	13,210
	6	14,859*	3,580	,000	7,672	22,046
4	1	19,527*	2,665	,000	14,177	24,876
	2	4,798*	2,203	,034	,375	9,222
	3	,305	2,928	,917	-5,572	6,183
	5	7,058*	2,011	,001	3,021	11,095
	6	15,164*	2,256	,000	10,635	19,694
5	1	12,469*	2,978	,000	6,490	18,447
	2	-2,260	2,578	,385	-7,435	2,915
	3	-6,753*	3,217	,041	-13,210	-,295
	4	-7,058*	2,011	,001	-11,095	-3,021
	6	8,106*	2,977	,009	2,129	14,084
6	1	4,362	3,525	,222	-2,715	11,439
	2	-10,366*	2,956	,001	-16,300	-4,432
	3	-14,859*	3,580	,000	-22,046	-7,672
	4	-15,164*	2,256	,000	-19,694	-10,635
	5	-8,106*	2,977	,009	-14,084	-2,129

Based on estimated marginal means

*. The mean difference is significant at the ,05 level.

b. Adjustment for multiple comparisons: Least Significant Difference (equivalent to no adjustments).

Table A4 7. Shapiro-Wilk' test of normality for the samples at different temperatures from 50 to 60 ºC, non-treated with the probe. To assume normality the significance (sig) needs to be superior to 0.050, df represent the degrees of freedom

Tests of Normality

	Kolmogorov-Smirnov[a]			Shapiro-Wilk		
	Statistic	df	Sig.	Statistic	df	Sig.
Temperature50_control	,196	52	,000	,916	52	,001
Temperature52_control	,181	52	,000	,877	52	,000
Temperature54_control	,201	52	,000	,878	52	,000
Temperature56_control	,101	52	,200*	,969	52	,189
Temperature58_control	,125	52	,043	,966	52	,136
Temperature60_control	,306	52	,000	,636	52	,000

*. This is a lower bound of the true significance.

a. Lilliefors Significance Correction

Table A4 8. Statistics description for samples at different temperatures treated with the probe. To assume normality the Skewness needs to be below 3 and the Kurtosis below 7

Descriptives

			Statistic	Std. Error
Temperature50_control	Mean		7,6596	,33051
	95% Confidence Interval for Mean	Lower Bound	6,9961	
		Upper Bound	8,3231	
	5% Trimmed Mean		7,5195	
	Median		6,6500	
	Variance		5,680	
	Std. Deviation		2,38336	
	Minimum		3,78	
	Maximum		14,82	
	Range		11,04	
	Interquartile Range		3,77	
	Skewness		,902	,330
	Kurtosis		,337	,650
Temperature52_control	Mean		6,4434	,11621
	95% Confidence Interval for Mean	Lower Bound	6,2101	
		Upper Bound	6,6767	
	5% Trimmed Mean		6,3703	
	Median		6,2475	
	Variance		,702	
	Std. Deviation		,83803	
	Minimum		5,38	
	Maximum		9,14	
	Range		3,76	
	Interquartile Range		,97	
	Skewness		1,419	,330
	Kurtosis		2,044	,650
Temperature54_control	Mean		6,5783	,22045
	95% Confidence Interval for Mean	Lower Bound	6,1357	
		Upper Bound	7,0208	
	5% Trimmed Mean		6,5997	
	Median		6,3300	
	Variance		2,527	
	Std. Deviation		1,58966	
	Minimum		1,61	
	Maximum		10,57	
	Range		8,96	

	Interquartile Range		,98	
	Skewness		,066	,330
	Kurtosis		2,288	,650
Temperature56_control	Mean		9,7263	,46369
	95% Confidence Interval for Mean	Lower Bound	8,7955	
		Upper Bound	10,6572	
	5% Trimmed Mean		9,5844	
	Median		9,3800	
	Variance		11,180	
	Std. Deviation		3,34371	
	Minimum		3,54	
	Maximum		18,54	
	Range		15,00	
	Interquartile Range		5,16	
	Skewness		,568	,330
	Kurtosis		,039	,650
Temperature58_control	Mean		10,7558	,35584
	95% Confidence Interval for Mean	Lower Bound	10,0414	
		Upper Bound	11,4702	
	5% Trimmed Mean		10,6588	
	Median		10,5450	
	Variance		6,584	
	Std. Deviation		2,56602	
	Minimum		4,49	
	Maximum		17,98	
	Range		13,49	
	Interquartile Range		2,63	
	Skewness		,606	,330
	Kurtosis		1,120	,650
Temperature60_control	Mean		6,6060	,29006
	95% Confidence Interval for Mean	Lower Bound	6,0236	
		Upper Bound	7,1883	
	5% Trimmed Mean		6,3318	
	Median		5,9450	
	Variance		4,375	
	Std. Deviation		2,09165	
	Minimum		3,09	
	Maximum		14,03	
	Range		10,94	
	Interquartile Range		,86	
	Skewness		2,461	,330

Kurtosis	6,190	,650

Table A4 9. Statistics information for the different temperatures treated with and without the probe

Paired Samples Statistics

		Mean	N	Std. Deviation	Std. Error Mean
Pair 1	Temperature50_probe	17,4862	52	21,29145	2,95259
	Temperature50_control	7,6596	52	2,38336	,33051
Pair 2	Temperature52_probe	32,2144	52	27,93157	3,87341
	Temperature52_control	6,4434	52	,83803	,11621
Pair 3	Temperature54_probe	36,7075	52	29,45062	4,08407
	Temperature54_control	6,5783	52	1,58966	,22045
Pair 4	Temperature56_probe	37,0129	52	21,79849	3,02291
	Temperature56_control	9,7263	52	3,34371	,46369
Pair 5	Temperature58_probe	29,9548	52	23,99845	3,32799
	Temperature58_control	10,7558	52	2,56602	,35584
Pair 6	Temperature60_probe	21,8485	52	17,95393	2,48976
	Temperature60_control	6,6060	52	2,09165	,29006

Table A4 10. Student's *t* Test between the samples with and without the probe for the different temperatures. There are extremely significant differences for pairs with a significance equal or below 0.001, df represent the degrees of freedom

Paired Samples Test

		Paired Differences					t	df	Sig. (2-tailed)
		Mean	Std. Deviation	Std. Error Mean	95% Confidence Interval of the Difference Lower	Upper			
Pair 1	Temperature50_probe - Temperature50_control	9,82654	20,73991	2,87611	4,05251	15,60057	3,417	51	,001
Pair 2	Temperature52_probe - Temperature52_control	25,77106	28,17049	3,90654	17,92834	33,61377	6,597	51	,000
Pair 3	Temperature54_probe - Temperature54_control	30,12923	29,78454	4,13037	21,83716	38,42130	7,295	51	,000
Pair 4	Temperature56_probe - Temperature56_control	27,28654	21,22050	2,94275	21,37871	33,19436	9,272	51	,000
Pair 5	Temperature58_probe - Temperature58_control	19,19904	24,23149	3,36030	12,45295	25,94513	5,713	51	,000
Pair 6	Temperature60_probe - Temperature60_control	15,24250	17,52042	2,42965	10,36478	20,12022	6,274	51	,000

Appendix A5. Detection limit experiments

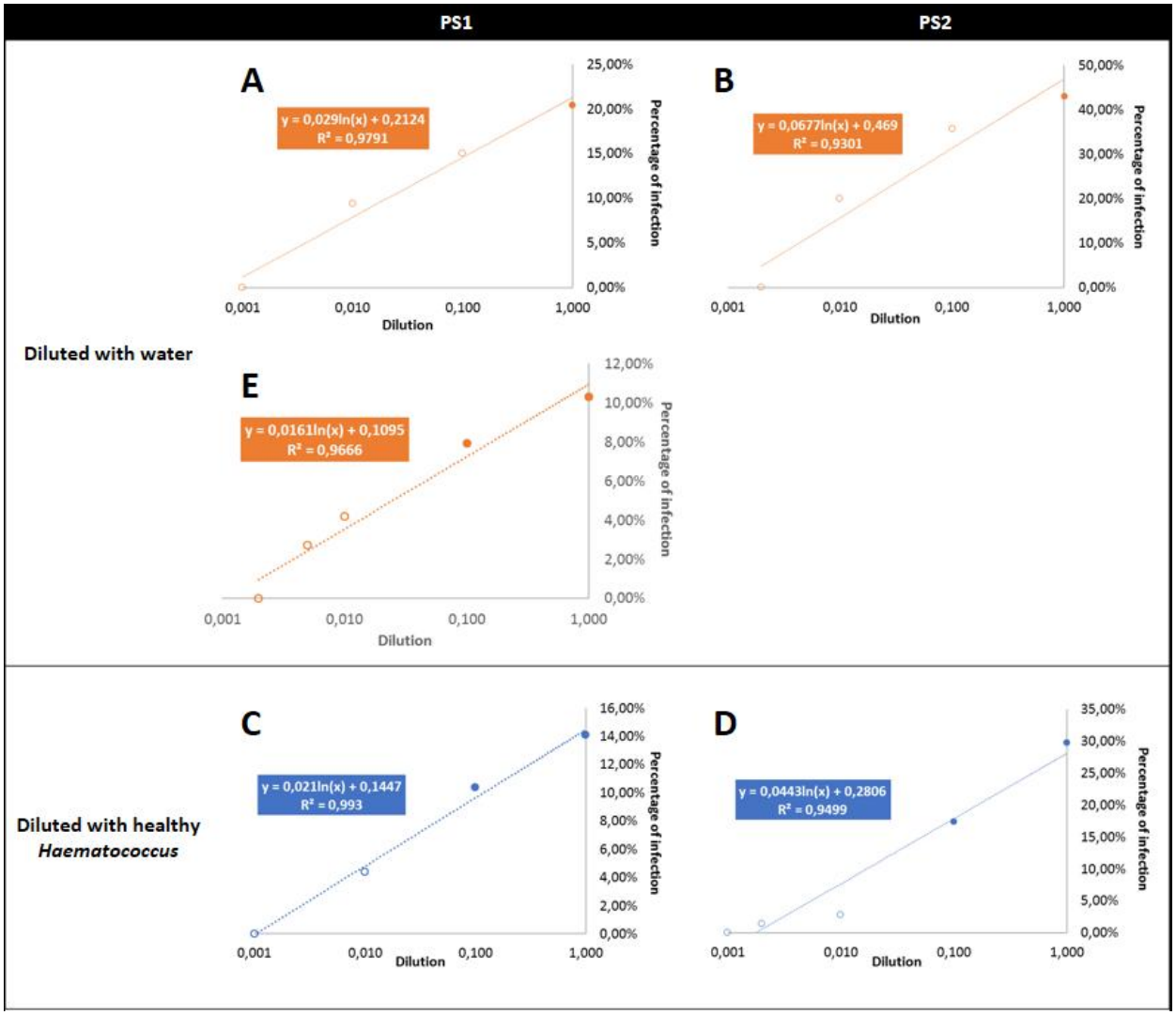

Figure A5 1. Dilution curves of *Haematococcus* infected cultures with PS1 and PS2 strains. The dilution series were done with water and with healthy *Haematococcus* cultures. The graphs express the percentage of infection (number of infected *Haematococcus* cells divided for the total number of *Haematococcus* cells). The counting was done in a Neubauer chamber. For every dilution, a different chamber was count for three times. The unfilled dots represent samples were the total number of *Haematoccocus* cells was inferior to 100. Every dilution was done with a x10 dilution factor, except for the data shown for B, D and E.

To find the detection limit, the dilution factor was calculated by matching the percentage of infection (y) to zero. Then, once the total number of infected cells at the original non-diluted series was known, it was multiplied by the dilution factor to find out the number of infected cells at the detection limit (Table A5 1).

Table A5 1. Detection limit [cells/mL] according to the calibration curves obtained and the value of total infected cells

Calibration curves obtained	Total number of *Haematococcus* cells/mL (non diluted)	Total number of infected cells/mL (non diluted)	Detection limit [cells/mL]
a) $y = 0.029 \ln(x) + 0.2124$	1.91×10^6	1.18×10^5	77
b) $y = 0.021 \ln(x) + 0.1447$	3.54×10^6	1.90×10^5	193
c) $y = 0.0677 \ln(x) + 0.469$	6.89×10^5	3.19×10^4	31
d) $y = 0.0443 \ln(x) + 0.2806$	4.72×10^6	1.27×10^5	225
e) $y = 0.0161 \ln(x) + 0.1095$	4.87×10^6	1.07×10^5	102

According to the results expressed at the Table A6 1, the detection limit is 126 ± 73 cells/mL for the concentrated sample. Applying the dilution factor (1:20) the detection limit will be 6 ± 4 cells/mL.